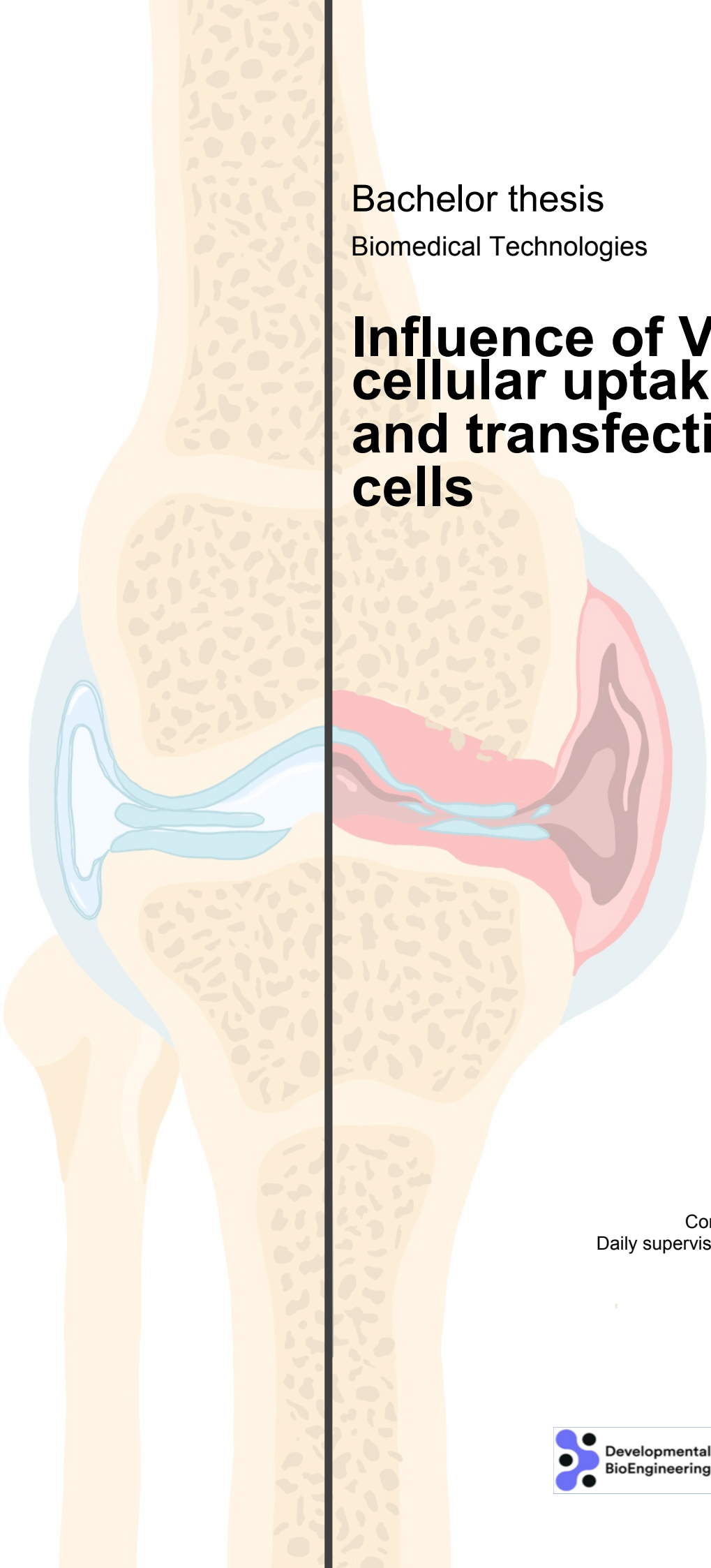

Bachelor thesis

Biomedical Technologies

Influence of VHH on cellular uptake of LNPs and transfection in joint cells

Maud Verhoeven
s2496720

July 10, 2024

Bachelor Thesis Committee:
Committee chair: prof. dr. M. Karperien
Daily supervisors: dr. J. Hendriks, dr. B. Zoetebier
External member: dr. R. Bansal

Developmental BioEngineering
Faculty of Science and Technology
University of Twente

Developmental BioEngineering | UNIVERSITY OF TWENTE. | TECHMED CENTRE

Contents

1 Abstract

Osteoarthritis (OA) and rheumatoid arthritis (RA) are the most common chronic degenerative joint diseases, that both primarly occur in the elderly population. In these diseases, synovitis occurs, in other words the inflammation of the synovium membrane. During inflammation, the synovium is a source of pro-inflammatory and catabolic products, leading to an imbalance between the cartilage synthesis and degradation. Currently there are two treatment pathways: non-pharmaceutical and pharmaceutical. The first involves weight loss and exercises. The second may involve surgery; this is usually done only in cases of meniscal damage. Intra-articular glucocorticoid injections can be given, but mainly relieve pain. Finally, NSAIDs can be prescribed to inhibit inflammation, but this is strongly discouraged in people with concurrent conditions, such as heart problems. The aim for the future is provide balance between the cartilage synthesis and degradation. This can potentially be achieved by target M1 macrophages using VHHs as targeting ligands on the LNPs containing miRNA, in which the miRNA causes reduced inflammation. This study will focus on a proof of concept, by looking at cellular uptake of LNPs containing plasmid DNA, in joint cells. The used VHH will target the IR-1L1 receptor. Therefore, chondrocytes known to contain IR-1L1 receptors were used for the proof of concept.

First, the LNPs were made with a microfluidic chip. Then three cell experiments were done. First, to look at cellular uptake and transfection in chondrocytes, with LNPs without VHH. Then also to look at cellular uptake and transfection with LNPs without VHH, but in macrophages. And lastly to look at specific cellular uptake and transfection in chondrocytes, with LNPs with VHH. In all three experiments, cellular uptake and transfection was looked at with EVOS microscopy and these photos were quantified with MATLAB. A presto blue assay was also done, to look at the toxicity of the LNPs.

Metabolic activity assays showed that both chondrocytes and macrophages retained similar activity up to 24 hours, but showed reduced activity after 96 hours, with transfection further reducing activity in chondrocytes. Cellular uptake shows higher uptake of LNPs in chondrocytes compared with macrophages, and higher concentration of LNPs led to higher uptake. However, addition of VHH to LNPs resulted in reduced uptake in chondrocytes. Transfection was observed in chondrocytes but not in macrophages, with higher LNP concentrations leading to higher transfection signals. Although, LNPs with VHH did not lead to transfection. Overall, VHHs affected the uptake of LNPs into joint cells opposite to expectations, suggesting that further research is needed to fully understand their influence on cellular uptake.

Furture research should take a look into another quantification of the EVOS microscopy picture, for example flow cytometry. In addition, the binding of VHH to cell receptors could be examined. In which it would be examined whether there is binding to the specific receptor first and then uptake, for example using a timelapse with EVOS microscopy. It would also be beneficial to look at the low uptake of LNPs with VHH by examining the properties of LNPs with compared to without VHH. Lastly, the future aim is to delivery drugs with the LNPs to specific cells. In this study the loaded LNPs seems to be more toxic to the cells than the non loaded LNPs. Follow-up studies should look into the toxicity of miRNA when inside the LNP.

2 Introduction

Osteoarthritis (OA) and rheumatoid arthritis (RA) are the most common chronic degenerative joint diseases, that both primarily occur in the elderly population. OA can arise when the joint is injured. Synovitis, the inflammation of the synovium membrane, occurs in these diseases[1, 2]. This membrane, a thin structure in the non-articulating surface of the joint, is a specialized tissue that is deformable, porous, and non-adherent to function in a mobile joint[3]. When the joint is injured the synovial membrane is a source of pro-inflammatory and catabolic products, including metalloproteinases (playing an important role in tissue repair) and aggrecanases (playing a role in the first stages of cartilage degeneration). These factors contribute to articular matrix degradation[4]. Due to this, there is a imbalance between cartilage synthesis and degradation [1]. To avoid this imbalance, the inflammation of the synovial membrane should be slowed down. Currently there are two treatment pathways, non-pharmaceutical and pharmaceutical. The first involves weight loss and exercise. In the case of the second, surgery may be performed; this is done mainly when the meniscus is affected. Intraarticular glucocorticoid injections are also a possible treatment, but only efficacious for short-term pain relief. In addition, nonsteroidal antiinflammatory drugs (NSAIDs) may be prescribed. Disadvantages are that this is strongly discouraged in people with concurrent conditions, such as heart problems [5]. This study will look at a new treatment method, which is targeted drug delivery.

2.1 Involved cells

Many cells are involved in osteoarthritis. First, cartilage and chondrocytes, with cartilage providing lubrication in the knee and chondrocytes supporting the cartilage by forming an extracellular matrix. Next, the synoviocytes, which are the cells present in the synovium. Lastly, an important cell type which is also the focus of this study, the immune cells, including monocytes and macrophages[6].

2.1.1 Monocytes and macrophages

Macrophages are the most common immune cells in the synovial membrane[6], which can provide the imbalance between cartilage synthesis and degradation (M1-M2 ratio), due to their role in the inflammation process. These cells evolve from monocytes. Monocytes are known as the second line of defense in the innate immune system and are circulating cells in the blood. They are recruited from the blood circulation into the synovial tissue by chemotaxis.

2.1.2 Types of monocytes

There are three types of monocytes: classical, intermediate and non-classical.

- The intermediate once will differentiate to pro-inflammatory macrophages (M1 macrophages) and contribute to synovial tissue inflammation. These can be recognized by a very high expression of CD14 and a low expression of CD16 (CD14++CD16-)[7].
- The classical monocytes can do this as well however, they can also differentiate to osteoclasts and cause bone erosion. These can be recognized by a high expression of CD14 and a high expression of CD16 (CD14++CD16+)[7].
- Lastly, the non-classical monocytes, these can also differentiate to pro-inflammatory macrophages, but these promote phagocytosis and resolution of inflammation (M2 macrophages). They can be recognized by a very high expression of CD14 and a high expression of CD16 (CD14++CD16+)[7].

The expressions mentioned above are not the only receptor genes that can be analyzed. Each monocyte has more specific receptor genes, which can be seen in figure 1 [7]. In OA and RA synovial joints, the classical monocytes are the most common and seem to be the circulating precursors of osteoclasts involved in bone erosion[7].

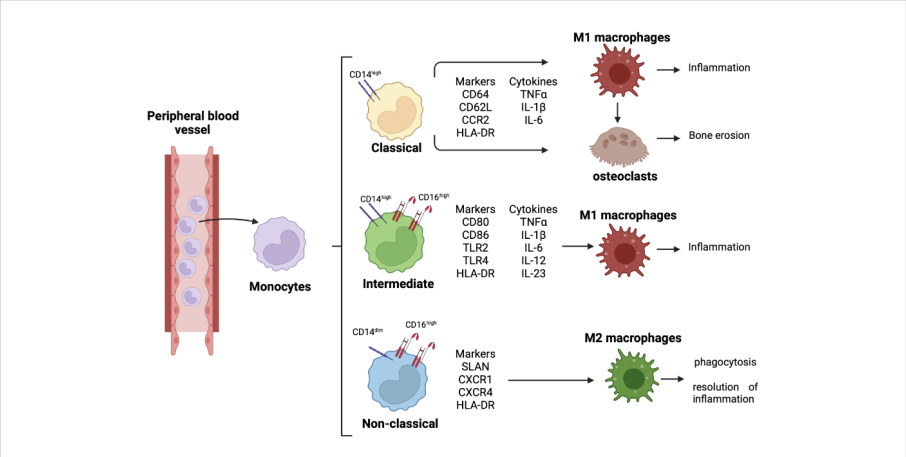

Figure 1: *Schematic representation of the different types of monocytes, their specific receptor genes and the macrophage type in which they differentiate with final function.*

2.1.3 Types of macrophages

Macrophages can also be divided in two types. First of, M1 macrophages, these are pro-inflammatory cells which are responsible for inflammation. Secondly, M2 macrophages, these regenerate by supporting proliferation, wound healing, and angiogenesis. They also moderate the inflammatory process. These two types can be kept apart by phenotype markers, which can be seen in table 1. They also secrete different cytokines and chemokines, which are also shown in table 1.

	Phenotype markers	Cytokines and chemokines
M1	HLA-DR (MHC class II), CD80, CD86, CD38, TLR4	Il-1β, IL-6, IL-12, IL-18, IL23, TNFα, CCR7, CCL2, HIF1α, ROS
M2	CD163, CD204, CD206, MerTK	IL-10, IL-4, IL-13, TGFβ, CCL4, CCL13, CCL17, CCL18

Table 1: *M1 and M2 macrophages have different phenotype markers and secrete different cytokines and chemokines.*

To slow down the inflammation of the synovial membrane, a balanced M1-M2 ratio should be achieved.

2.2 Medication

To get balance between the M1 and M2 macrophages, medication that can inhibit M1 macrophages or activate M2 macrophages can be used. A good way to do this is mRNA or miRNA.

2.2.1 miRNAs

MicroRNAs (miRNAs) are small non coding RNAs, found in both introns and extrons. Their function is, post-transcriptionally regulating gene expression, leading to controlling the kinds and amounts of proteins that will be made. [8, 9]
There are a lot of miRNAs that regulate the polarization of M1 and M2 macrophages. They can also regulate the macrophage phenotype during the progression of various diseases [9].
In M1 macrophages the following miRNAs are important when focusing on the inflammation process. [8]

- miR155: this one has a role in inflammatory signaling, by promoting pro-inflammatory responses. It also inhibits M2 polarization.[10, 11]
- miR9: this can suppress the anti-inflammatory response [11]
- miR127: this one promotes the M1 polarization, inhibits M2 polarization and promotes pro-inflammatory responses [11]
- miR125b: this one enhances the pro-inflammatory responses [11]

In most studies miR155 emerges as the most important in the inflammation process.[10, 11, 9, 8]

2.3 Nanoparticles

To get nucleic acids, like miRNA or mRNA, into the cell where it can do its work, an encapsulation is needed. Due to unstable nature of nucleic acids degradation will occur when exposed to blood, before it reaches the cell [12, 13, 14]. There are many biologically derived and chemically based materials that have been successful in transporting nucleic acids to the preferred cell. Biologically derived nanoparticles include exosomes, bacteria outer membrane and virus-like particles. Chemically based materials include many polymer and lipid based nanoparticles (LNPs). These are used because of their high potency and diversity. For mRNA delivery, lipid nanoparticles is believed to be the first option, as many studies have demonstrated efficacy [13, 15]. This method is also already being used for several diseases such as cancer immunotherapy, virus vaccines and gene editing [14].

2.3.1 Types of LNPs

Lipid nanoparticles are lipid based vesicles, they can potentially be used for the delivery of drugs. They can act as a protective encapsulation for nucleic acid load, by preventing enzymatic degradation until the load enters the cell [16]. Their exists four different types of lipid nanoparticles: liposomes, solid lipid nanoparticles (SLNs), nanostructured lipid carriers (NLCs) and hybrid lipid-polymeric nanoparticles, shown in figure 2 [17].

Liposomes
Liposomes have a spherical structure and consist of an amphipathic phospholipid bilayer and an internal aqueous core. This is suitable for both hydrophilic and hydrophobic molecules. Where the hydrophilic molecules will be in the aqueous phase of the core and the hydrophobic in the lipophilic bilayers of the shell [17].

Solid lipid nanoparticles (SLNs)
SLNs also have a spherical structure and are made of a solid fully crystallized lipid matrix. A subdivision can be made of three types of SLNs: 1) solid solution model (without drug in it), 2) drug-enriched shell model (with the drug around the shell), and 3) drug-enriched core model (with the drug in the middle). Their advantages are stability, excellent drug protection and controlled release. However, there are drawbacks too, such as low drug-carrying capacity and poor long-term drug retention [17].

Nanostructured lipid carriers (NLCs)
NLCs is a successor of the SLNs, where the solid component is substituted by a liquid component. This results in a larger drug corporation space. The structure of the NLCs can be described by three types: 1) imperfect crystal type, 2) multiple type (where the drug is encapsulated by an oil-layer), and 3) amorphous type (homogeneous amorphous) [17].

Hybrid lipid-polymeric nanoparticles
Hybrid lipid-polymeric nanoparticles is a combination of two types of materials. It comprises a therapeutic-containing polymeric core enveloped by an inner lipid layer and a PEGylated lipid outer layer. Because of this it has properties of both materials and makes it very stable and greatly biocompatible [17].

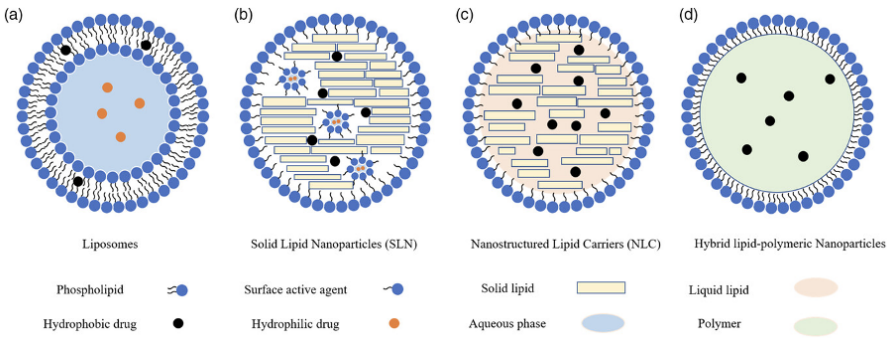

Figure 2: *Schematic view of the four different types of LNPs. a) liposome with spherical structure consists of an amphipathic phospholipid bilayer and an internal aqueous core, b) SLNs, also with spherical structure and made of a solid fully crystallized lipid matrix, c) NLCs, a successor of the SLNs, where the solid component is substituted by a liquid component, d) Hybrid lipid-polymeric nanoparticles, a combination of two types of materials[17].*

2.3.2 Formulation

LNPs mostly consists of ionizable lipids, PEGylated lipids, phospholipids and cholesterol [14, 18].

- Ionizable lipids are good for RNA therapeutics. At low pH, the LNPs are positively charged, which is good to encapsulate the negatively charged RNA and the charge becomes less positive or almost neutral at physiological pH, to reduce toxicity [14].
- Phospholipids are helper lipids, which provide structural stability and can lead to disruption of the lipid bilayer.
- Cholesterol is also used to reach particle stability.
- PEGylated lipids have various roles, for example stability and decrease in aggregation. It also prolongs blood circulation time and protects the surface [14].

2.4 Cellular uptake

When a nanoparticle (NP) reaches the cell, it will react with the exterior membrane and can be taken up by multiple mechanisms. Entering the cell will mainly go through endocytosis, leading to engulfment of LNPs in membrane invaginations. The formed endocytic vesicle will then be transported to specialized intracellular sorting/transportation compartments [19]. Endocytosis can be classified into several types, depending on cell type, proteins, lipids, and other molecules involved in the process.[19]

2.4.1 Phagocytosis

Phagocytosis occurs mainly in phagocytic cells, such as macrophages, monocytes, neutrophils and dendritic cells. An important initiator for phagocytosis is opsonization. In this process, opsonins are adsorbed to the surface of a NP. Examples of opsonins are immunoglobulins, complement proteins, or other blood proteins. Opsonized NPs will be recognized by the phagocytic cells and than attached via specific ligand-receptor interactions. After this, engulfment takes place and a so-called 'phagosome' is made, shown in figure 3 [19].

2.4.2 Clatherin-mediated endocytosis (CME)

Clatherin-mediated endocytosis occurs either via receptor-specific uptake or via non-specific adsorptive uptake. The last one referred to receptor-independent CME, in this case uptake takes place without direct binding with membrane components. CME is the most important mechanism for cells to get nutrients and plasma membrane components. This mechanism takes place at the plasma membrane, rich of clathrin, as shown in figure 4 [19].

2.4.3 Caveolae-dependent endocytosis

Caveolae-dependent endocytosis has an important role in many biological processes, for example cell signaling and regulation of lipids. It occurs in epithelial and non-epithelial cells and form a flask-shaped membrane invagination, as shown in figure 5 [19].

2.4.4 Macropinocytosis

Macropinocytosis is a unique form of the pinocytosis process. The difference is that it does not involve the utilization of lipid rafts or pit-forming proteins. In this case, as a result of the cytoskeleton rearrangement, large membrane extensions or ruffles are formed. These extensions fuse back on the membrane and form a large vesicle, as shown in figure 6. All particles and dissolved molecules in the extracellular fluid are taken into the vesicle, which lead to a form of non specific uptake [19].

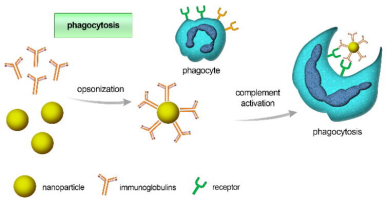

Figure 3: *Schematic view of the mechanism of phagosytosis*

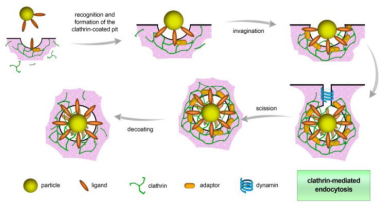

Figure 4: *Schematic view of the mechanism of clathrin-mediated endocytosis*

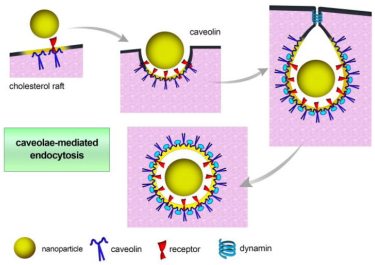

Figure 5: *Schematic view of the mechanism of caveolae-dependent endocytosis*

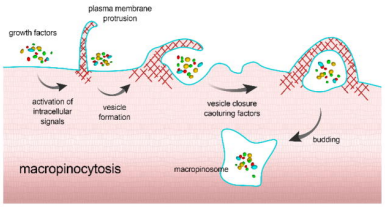

Figure 6: *Schematic view of the mechanism of macropinocytosis*

In OA and AR, primarily the macrophages and monocytes are important and will be targets of the nanoparticles. Therefore, this will mainly involve phagocytosis.

2.5 LNP targeting

To target specific cells, a biomolecule can be added to the surface of the LNP. Different types of biomolecules are peptides, antibodies or antibody fragments, aptamers and small molecule targeting. [20]

2.5.1 Antibodies or antibody fragments

For targeted drug delivery, antibodies, or immunoglobulins (Ig), are the first macromolecular ligands. These are large glycoproteins that can be used to target receptors or antigens. They are also involved in processes like opsonization, phagocytosis, and antibody-dependent cytotoxicity [21]. Their exist four types of Igs, of which IgG is the most common in humans. IgGs consists of four protein chains, two light chains and two heavy chains which form a 'Y' shape [22].

2.5.1.1 VHH

Not only the full antibody, but also an antibody fragment can be used for specific targeting of receptors. These are parts of antibody domains and will always have a variable domain, so specific binding will still be possible. A nowadays used antibody fragment is the variable heavy domain of the heavy chain only antibody (VHH), also known as nanobody. [22]. This is a unique type of antibodies found in camelids. A major advantage of these antibodies is that they retain their full antigen specificity at about 15kDa. In addition, they can be easily humanized [23]. In figure 7 both the full antibody and an antibody fragment is shown.

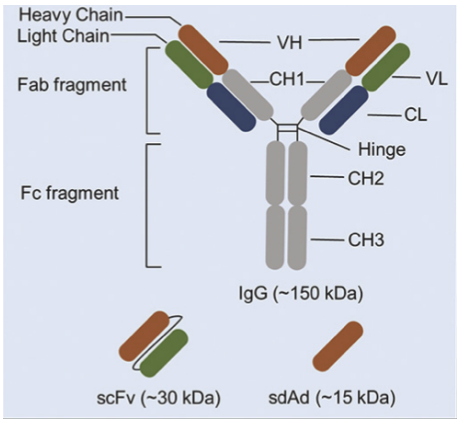

Figure 7: *Schematic view of the full antibody (on top) and an antibody fragment (on bottom, in brown)[21]*

2.5.2 Peptides

Peptides are small, synthetic molecules. They are more stable than antibodies and unlikely to be immunogenic. A disadvantage is the fast degradation within the body. Arginylglycylaspartic acid (RGD) is the most commonly used peptide, expecially to target cancerous cells [20].

2.5.3 Aptamers

Aptamers are biomolecules made of nucleic acids consisting of single-stranded DNA, RNA or unnatural oligonucleotides. This will form unique structures and leads to specific targets with high affinity and specificty [20].

2.5.4 Small molecule targeting

Small molecules are mostly used because of their low cost and easy production. Examples of these small molecules are folic acid and sugar molecules [20].

2.6 Aim of this study

The aim for the future is to target M1 macrophages using VHHs as targeting ligands on the LNPs containing miRNA. In which case the miRNA will ensure that reduced inflammation will take place. The reduced inflammation prevents imbalance between cartilage synthesis and degradation.
In this study, the aim is to make a proof of concept for the cellular uptake of the LNPs containing plasmid DNA. The used VHHs target the IR-1L1 receptor. Therefore, chondrocytes known to contain an IR-1L1 receptor were used for this proof of concept. LNPs are used because of their low immunogenicity, biodegradability and high payload capabilities of nucleic acids [17]. In doing so, the use of ionizable lipids will make them controllable under different pH conditions [14]. For targeting the cells, VHHs are used because they are small and still retain their full antigen specificity. In doing so, they are also easy to humanize.
This leads to the research question: **What is the influence of targeting with VHHs on the uptake of LNPs and transfection in joint cells?**

LNPs with VHHs are expected to give higher uptake than LNPs without VHHs. Because the VHHs are specific to the cells used, they will be recognized. This recognition will lead to phagocytosis. The LNPs without VHHs can also be incorporated. This will be non-specific uptake, so it will not be via phagocytosis, but for example via macropinocytosis.

3 Materials and methods

3.1 Lipid nanoparticle fabrication and characterisation

3.1.1 Lipid nanoparticle fabrication

To make the LNPs, a mixture of lipids consisting of ionizable lipid (Dlin-MC3-DMA: BLD pharmatech GmbH; catalogue No. BD00786192-1g, 20 mg/mL), phospholipid (DSPC: Avanti polar lipids, Inc, 10 mg/mL), cholesterol (Signma Aldrich, 10 mg/mL), PEG-lipid (DMG-PEG2000: 10 mg/mL) and fluorescent Cy5.5 for LNP locating (PEG-lipid-Cy5.5: Avantu polar Lipids, Inc, 1 mg/mL) was first made, in a molar ratio 50:10:38.3:1.4:0.2:0.1, respectively. Another mixture is then made, consisting of tRNA (Thermo Fisher Scientific) or mCherry (0.095 mg/ml) dissolved in sodium acetate buffer (100mM, pH 4).

Then the two mixtures were mixed using a microfluidic chip. In this process, two syringes were connected to the inlets of the chip using 1 mm diameter tubing and connectors. There was also tubing connected to the outlet to collect the mixture in an brown eppendorf, to protect the mixture from light. The two syringes were used to combine the two mixtures in a 3:1 tRNA/mCherry:lipid flow rate ratio (v/v) at a total constant 1mL/min flow rate. The outcome was purified by dialysis with a 50kDa MWCO filtration membrane in an excess of MilliQ, for at least 1h. This removed ethanol, resulting in a solution of the LNPs in MilliQ. Before use, particles need to be spin filtered using a Vivaspin spin filter, to prevent aggregation.

3.1.2 Lipid nanoparticle characterization

For characterisation of the LNPs, DLS (dynamic light scattering) is used, determing the size. For this measurement, the LNPs were diluted in PBS and transferred into a disposable cuvet. To ensure a reliable measurement, there must be at least 50 LNPs in the measured sample.

3.1.3 DNA assay

A DNA assay was done with QuantiFluor® dsDNA System (Product E2670), to asses if mCherry is on the inside of the LNP rather than the outside. First, 1X TE Buffer solution was prepared, by diluting the 20X TE Buffer 20-fold with nuclease-free water. Subsequently, the working solution was prepared, by diluting the QuantiFluor® dsDNA Dye 1:400 in 1X TE buffer. Also a standard curve was prepared, using dsDNA standards, that resulted in 0.05–200ng/well. After all the solutions were prepared, 200µl of QuantiFluor® dsDNA Dye working solution was added to each well. Then 10µl of the standard curve solutions and the solution to be measured were each added to a well. The plate was well mixed, incubated for 5 minutes and protected from light. Finally, the plate was measured with VICTOR Microplate Reader for fluorescence (504nm - extinction and 531nm - emission).

3.1.4 SDS-page

To determine if the coupling between the loose VHH and the lipid was successful, SDS-PAGE with Coomassie blue staining was performed. The SDS-PAGE samples were prepared by mixing 2µg of the sample with 5µg sample buffer (β- mercaptoethanol 1:9 Laemmli sample buffer) and the volume was supplemented to 20µL with PBS. The samples were then heated to 95 °C for 5 min and spin-filtered.
The gel tank was prepared by filling it with a 1x solution of the 1x SDS running buffer diluted with demi water. Then, after loading the 4-15% Bio-Rad pre-cast gel into the tank, 20µL of all samples were loaded into the gel. In the outer lanes, 5µL protein ladder was added. The measurement was performed at 100V for 20 min and 160V for 40 min, after which the gel was rinsed with MilliQ and placed overnight in a container with fixation buffer (50% methanol, 10% acetic acid, 40% demi water).
Lastly, the gel was stained with Coomassie staining solution (fixation solution and 0.25 % w/v Coomassie Blue R-250) for 2-4 hours on a shaker. Destaining of the gel was done with a destaining solution (5% methanol, 7.5% acetic acid and 87.5% H_2O) for 2-4 hours, with refreshing every 30 minutes, for at least the first two hours. Finally, the gel was imaged with FluorChem M system from ProteinSimple.

3.1.5 Surface plasmon resonance assay (SPR)

To look at the interaction between the human IR-1L1 receptor and both loose VHH and VHH bound to the lipid, SPR analysis was performed. First, the sensor was prepared. Here, the IR-1L1 receptors were immobilized for 30 minutes on G-type easy2spot sensors via reaction to free amines using the Wasatch microfluidics continuous flow spotter (Wasatch Microfluidics, Salt Lake City, UT, USA). This reaction was performed in 50 mM acetic acid buffer (150 µL per spot) with different concentrations of antibody.
An immobilization buffer of pH 4.6 provided protein coupling with the highest retained activity and was therefore used for all experiments. This pH ensures concentration of antibodies on the negatively charged hydrogel. In addition, the low pH reduces the reactivity of lysines, providing more targeted coupling to primary amines.

The sensor is deactivated intermediately with 1% BSA in 50 mM acetate buffer at pH 4.6 for 7 min and then with 0.2 M ethanolamine at pH 8.5 for another 7 min to reduce nonspecific interactions.

The IBIS MX96 (IBIS Technologies, Enschede, The Netherlands) was used for the measurements. The device uses an angle scan method with automatic adjustment to determine SPR shifts. It has an automatic fluid handling system and uses back-and-forth flow through a microfluidic flow cell that fits on the array to allow minimal sample utilization. The device uses SUIT software (IBIS Technologies, Enschede, Netherlands) for measurements, in which the type of interaction, interaction times, samples and regions of interest (ROIs) for the antibodies were set. A template was also created and loaded into the IBIS software for data processing. Once programmed, the machine is ready for automatic liquid handling and SPR angle measurements. Forty-eight sensor points were used. The reciprocating flow was set at 10 µL/min in a flow cell with 12 µL of sample. Sprint software was used for data collection.

Affinity was measured by the kinetic titration method to avoid possible reduction of binding capacity under regeneration conditions.
Human, canine and equine IL-1R1 were spotted at 260, 130 and 65nM with 4 spots per concentration. Next, VHH or lipid-VHH were dissolved in system buffer containing PBS with -0.075% Tween80 at a concentration of 16.25, 32.5, 65, 130 and 260nM. Kinetic titration was performed as follows: first, a blank was injected, followed by the respective VHH or lipid-VHH at 16.25 nM and successive injections of two times increased concentrations to 260 nM. The association time of each interaction was 10 min followed by an 8 min dissociation. Between each injection, the sensor was washed with system buffer.

3.2 Cellular uptake and metabolism

3.2.1 Cell culture

Chondrocytes (SW1353) were used for the first and third experiment. They were cultured with high glucose Dulbecco's modified Eagle's medium (DMEM)(ThermoFisher Scientific, Waltham, MA, USA; catalogue No. 11965-092) with 4 mM l-glutamine, 10% fetal bovine serum (Thermo Fisher Scientific, Waltham, MA, USA; catalogue No. 10270-106) and 1% penicillin–streptomycin antibiotic solution (Thermo Fisher Scientific, Waltham, MA, USA; catalogue No. 15140-122) at 37 °C and 5% carbon dioxide conditions. The cells within passage 4 to 8 were used in these experiments.
To get the cell suspension, trypsin was added and the cells were incubated for six minutes at 37°C. Culture medium was added to neutralize the trypsin (Sigma-Aldrich, catalog number: T3924-100 ml).

During the second experiment the THP-1 cell line was used, these are human monocytic cells obtained from an acute monocytic leukemia patient. These cells were cultured in RPMI 1640 w/L-Glutamine-Bicarbonate (Sigma-Aldrich, catalogue No. R8758), 10% fetal bovine serum (Thermo Fisher Scientific, Waltham, MA, USA; catalogue No. 10270-106) and 1% penicillin–streptomycin antibiotic solution (Thermo Fisher Scientific, Waltham, MA, USA; catalogue No. 15140-122) at 37 °C and 5% carbon dioxide conditions. The cells from passage 15 were used in this experiment.
To obtain a cell suspension of these cells, a cell palette must be obtained with centrifugation at 1200 rpm for 5 minutes.

The cells were cultured in 96-wells plate (Greiner bio-one) in a cell suspension of $\sim$10,000 cells/cm2 for the SW1353 cells and $\sim$12.500 cells/cm2 for the THP-1 cells, at day zero. For the first and second experiment, two 96-wells plates were used. One for the presto blue measurement and one for the measurement with EVOS. For the third experiment four 96-wells plates were used. Two for the presto blue measurements and two for the measurement with EVOS.

One hour after the THP-1 cells were seeded, they had to be treated with lipopolysaccharide (LPS). THP-1 cells are suspension cells and this treatment makes them settle to the bottom, which is necessary for the experiments being done. Also, the treatment causes the cells to differentiate, which can promote uptake.

For the third experiment, it was necessary to block the cells in two plates. Approximately four hours after seeding the SW1353 cells, loose VHH was added to the culture to block these receptors.

Phase contrast microscopy using Nikon (eclipse TS100) was used before every experiment to examine the confluence and morphology of the cells. To analyse the cell viability and count the cells, an EVE (NanoEnTek) was used.

3.2.2 Transfection

At day one, the cells were transfected. When LNPs were in the culture, medium is used without penicillin–streptomycin antibiotic solution (Thermo Fisher Scientific, Waltham, MA, USA; catalogue No. 15140-122).
For the first experiment two types of LNPs were used, empty LNPs and LNPs with plasmid, mCherry inside. Those LNPs were added to the cells in three different concentrations, 40-400-4000 dilution series. For the second experiment, the mCherry LNPs were used again and instead of the empty LNPs, LNPs with tRNA were used. For this experiment the same dilution series is used as before, 40-400-4000x.
For the third experiment, LNPs with mCherry inside were used compared to LNPs with mCherry inside and an antibody, VHH on the surface. This time, the LNPs were added in two different concentrations, 40-400 dilution series. The controls used in these experiments were, lipofectamine as positive control. As negative control, only plasmid (without LNP) was used for the EVOS measurement and only medium (without cells) for the presto blue measurement. For the presto blue measurement, also only cells was included as control.

3.2.3 Cell metabolism

To determine the cell metabolism, presto blue assay was used. First, the medium was removed and then a 1:10 dilution of presto blue with culture medium (without penicillin–streptomycin antibiotic solution) was added and the cells were incubated for 16 minutes 37°C and 5% CO2. The cell metabolism was measured with the VICTOR Microplate Reader (560nm excitation, 590 emmision).
This test was done for the first and second experiments at three time points, at 4, 24 and 96 hours after adding the LNPs. For the third experiment, the test was done at four time point, at 2, 4, 6 and 24 hours after adding the LNPs.

3.2.4 Cellular uptake

To measure the cellulare uptake, EVOS Cell Imaging Systems was used. The Cy5 filter (628/40nm excitation, 692/40 emmission) was used for the Cy5.5 signal, to locate the LNPs, the TX Red filter (585/29nm excitation, 624/40nm emmission) for the mCherry signal, to see if transfection has occured and transmission to locate the cells. To prepare the cells, first the medium was removed, then the cells were washed three times with Dulbecco′s Phosphate Buffered Saline (Sigma-Aldrich, catalogue No.PBS2541) and lastly new medium was added, in which the cells were also seeded.
Washing the cells was done at three time points in the first two experiments, at 4, 24 and 96 hours after adding the LNPs, and then the cells were observed using the EVOS at all time points from the time they were washed. For the third experiment four time points were used (2, 4, 6 and 24 hours).

3.3 Quantification of cellular uptake

A MathWorks Matlab script was used to determine the uptake quantification of the EVOS images, which isolated the red channel from the RGB image. From this data the amount of red pixels were counted, a pixel was seen as red when the RGB value lied between 20 and 255. The lower limit of this can vary between 20 and 150, as background noise was much higher in some images.
These results assumes that each well contains the same number of cells because the seeding density is the same everywhere. The script is in appendix A.

4 Results

4.1 Lipid nanoparticles

The production of nanoparticles resulted in a yield, high enough for all required experiments.

4.1.1 Size and PDI

The size and PDI of these LNPs are shown in table 2. Almost all the LNPs are about the same size, except for the LNPs with tRNA inside. These LNPs are 50 to 60nm larger. Also the PDI of these LNPs is bigger than the others, which means these are less stable.

Table 2: Size of used types of LNPs measured with DLS

	empty LNPs	tRNA LNPs	mCherry LNPs (first batch)	mCherry LNPs (second batch)	mCherry LNPs with VHH
Size (µm)	135.3 ± 3.30	212.2 ± 24.3	143.0 ± 1.68	122.3 ± 1.0	123.3 ± 1.2
PDI	0.29 ± 0.02	0.56 ± 0.10	0.24 ± 0.01	0.25 ± 0.01	0.15 ± 0.01

4.1.2 DNA assay

In figure 8, on the left, the calibration curve of the DNA assay is shown. On the right, the results of the complete and degraded LNPs, and loose mCherry is shown. The complete LNPs gave a signal of 68369, which will give a concentration of ±74ug/ul. The same condition, but ten times diluted, gave a signal of 1798, which will give a concentration of ±1,2ug/ul. For the degraded LNPs the signal is 19862 and for the ten times diluted condition a signal of 2883, which will give the concentrations ±19ug/ul and ±2,8ug/ul, respectively. Also loose mCherry is measured and this gave a signal of 404, which will give a concentration of ±0,005ug/ul.

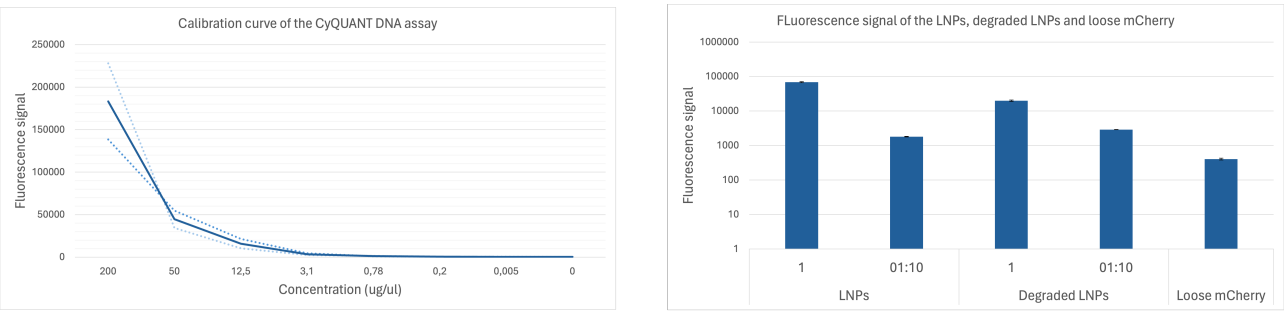

Figure 8: *Results of the DNA assay, with left a calibration curve made with dsDNA and right the results of the complete and degraded LNPs, and loose mCherry*

4.1.3 SDS page

SDS page was done to show that the coupling between the lipid and VHH was successful. The first column shows the loose VHH, which gives a signal at 15kDa. This signal is also seen in the rest of the columns, which means that in none of the columns is the loose VHH fully reacted. The second column shows the lipid VHH, as already mentioned the loose VHH can still be seen here. Also a dash at 25kDa can be seen, showing the coupling. The fourth column shows the blocked lipid and it shows no signal at 25kDa. The control in the sixth column, with the 8-PEG-arm, gives multiple bands between 100kDa and 150kDa, showing reaction.

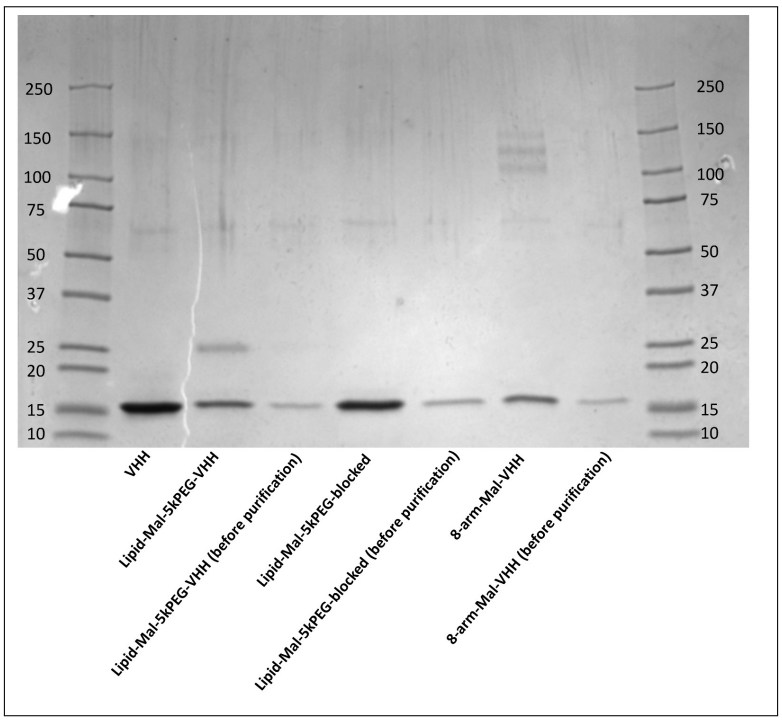

Figure 9: *SDS page with the successful coupling between the lipid and VHH. With loose VHH, blocked lipid-VHH and 8-arm PEG as controls.*

4.1.4 Surface plasmon resonance assay (SPR)

In figure 10 the results of the SPR are shown. The grey line gives the results of the human IR-1L1 receptor, the red line of the canine and dark green one of the equine. The left figure shows the measurement with the loose VHH and the right figure the measurement with the lipid-VHH. In both cases, interaction can be seen. In the right figure, the signals are slightly weaker than in the left figure. Both the canine and equine did not give a clear signal.

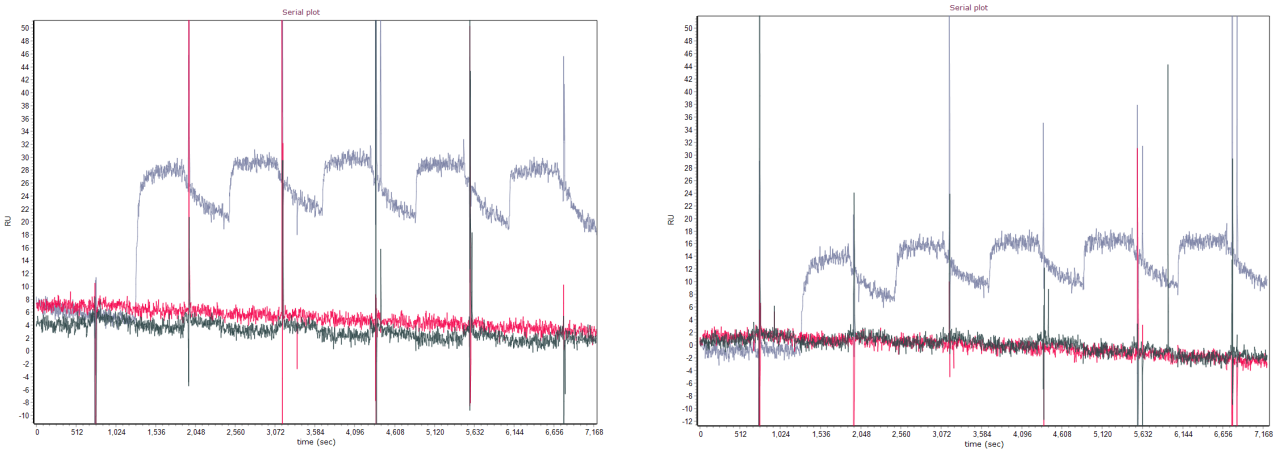

Figure 10: *SPR results of the loose VHH (on the left) and the lipid-VHH (on the right) with an IR-1L1 receptor, and canine and equine as controls.*

4.2 Cell metabolism

In figure 11 the results of the first experiment are shown. In this experiment chondrocytes (SW1353) were used, with empty and mCherry LNPs in a dilution series of 4-40-400x. After 4 and 24 hours the metabolic activity are slightly lower than the control with only cells. After 96 hours, the metabolic activity for the high concentration is much lower than the control with only cells. This shows that this concentration is toxic to cells. Therefore, based on this result, the dilution series was adjusted to 40-400-4000. This new range was used for the rest of the experiments.

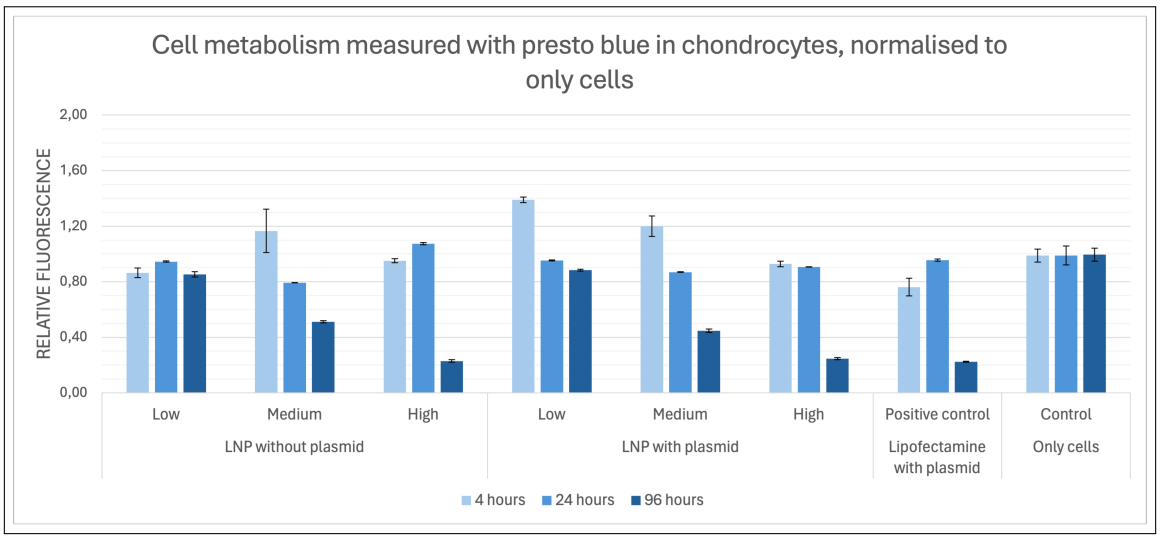

Figure 11: *Cell metabolism results measured with presto blue in chondrocytes (SW1353) cells with empty and mCherry LNPs, at three different time points (4, 24 and 96 hours) in a dilution series of 4-40-400x. The values are normalized to the control with only cells.*

The measurements for cell metabolism with presto blue was done for the next three experiments and is also shown in bar graphs. The negative control of only medium, in all cases, gave a low fluorescence signal and all graphs are normalized to the control with only cells. The results before normalizing can be seen in appendix B

4.2.1 Empty and mCherry LNPs in chondrocytes (SW1353)

For the first experiment the results are shown in figure 12. It is clearly seen that after four hours the cell metabolism is for all conditions approximately the same and around one, the cell metabolism in the control with only cells. After 24 hours the cell metabolism is slightly lower, indicating the LNPs are slightly toxic to the cells. For the cells with empty LNPs the concentration seems to have no effect on cell metabolism, because the bars are almost all about the same. For the cells with mCherry LNPs, a higher concentration seems to result in lower cell metabolism. These two observations are also reflected after 96 hours. What can also be seen after 96 hours is that at medium and high concentration, cell metabolism is again higher than after 24 hours. The control, lipofectamine, shows a decreasing cell metabolism over time, indicating that it is slightly toxic to the cells.

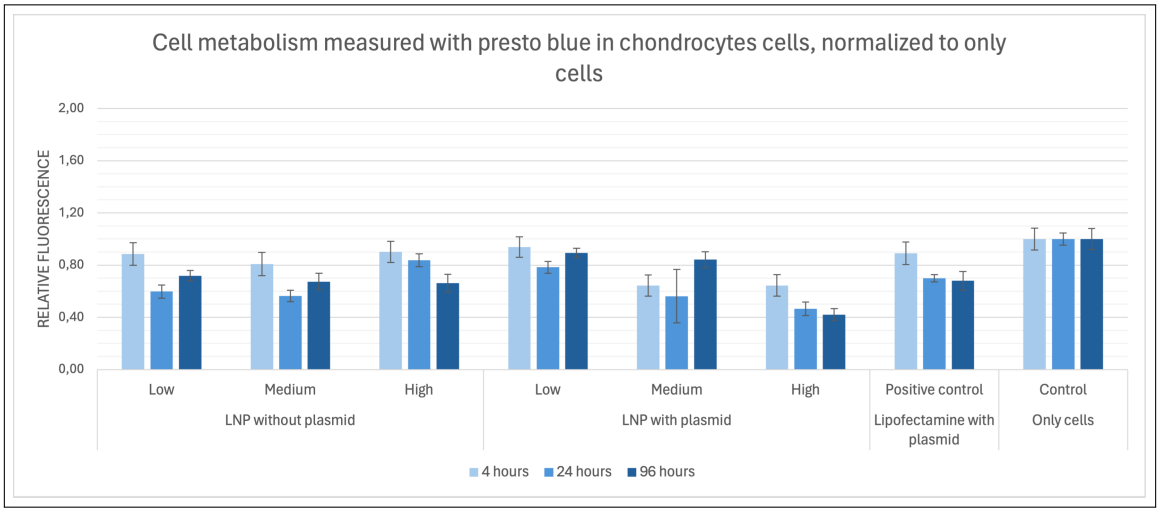

Figure 12: *Cell metabolism results measured with presto blue in SW1353 cells with empty and mCherry LNPs, at three different time points (4, 24 and 96 hours) in a dilution series of 40-400-4000x. The values are normalized to the control with only cells.*

4.2.2 tRNA and mCherry LNPs in macrophages (THP-1)

For the second experiment, with tRNA and mCherry LNPs in macrophages (THP-1), the results are shown in figure 13. After 4 and 24 hours, almost all the bars are about the same height and around zero, which lead to a metabolic activity almost the same as for only cells. After 96 hours, all bars are lower than the control with only cells, indicating that the LNPs are slightly toxic to this cells.

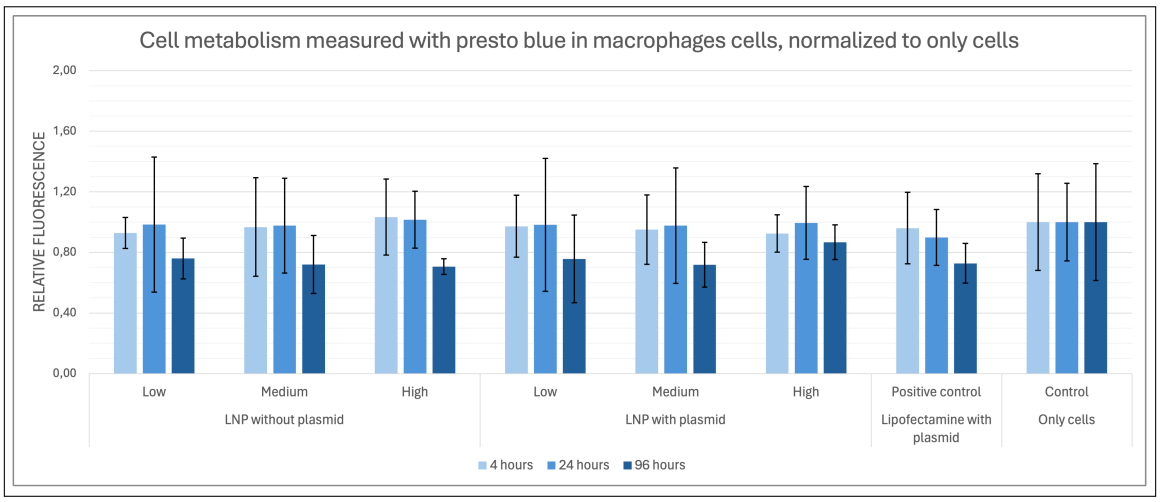

Figure 13: *Cell metabolism results measured with presto blue in THP-1 cells with tRNA and mCherry LNPs, at three different time points (4, 24 and 96 hours) in a dilution series of 40-400-4000x. The values are normalized to the control with only cells.*

4.2.3 mCherry LNPs with and without VHH chondrocytes (SW1353)

For the last experiment, again chondrocytes (SW1353) were used, with mCherry LNPs with and without VHH on the surface. In figure 14 the results of the non blocked chondrocytes are shown. In this case the metabolic activity in the cells stay around the the control with only cells. Only after 24 hours in the cells to which LNPs with VHH are added a greater difference can be seen, there the metabolic activity is higher.

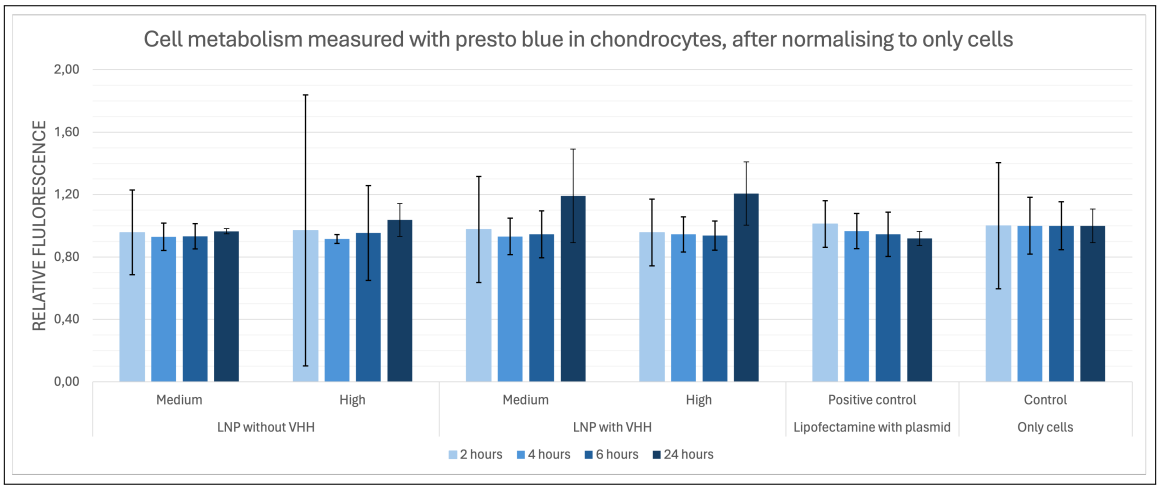

Figure 14: *Cell metabolism results measured with presto blue in chondrocytes (SW1353) at four different time points (2, 4, 6 and 24 hours). Normalized to control with only cells.*

In figure 15 the results of the blocked chondrocytes (SW1353) are shown. In this case the same trend can be seen, as in figure 14 with the non blocked cells. The cell metabolism is in almost all cases about the same as the control with only cells. Except after 24 hours, their the metabolic activity is higher for the cells to which LNPs with VHH are added.

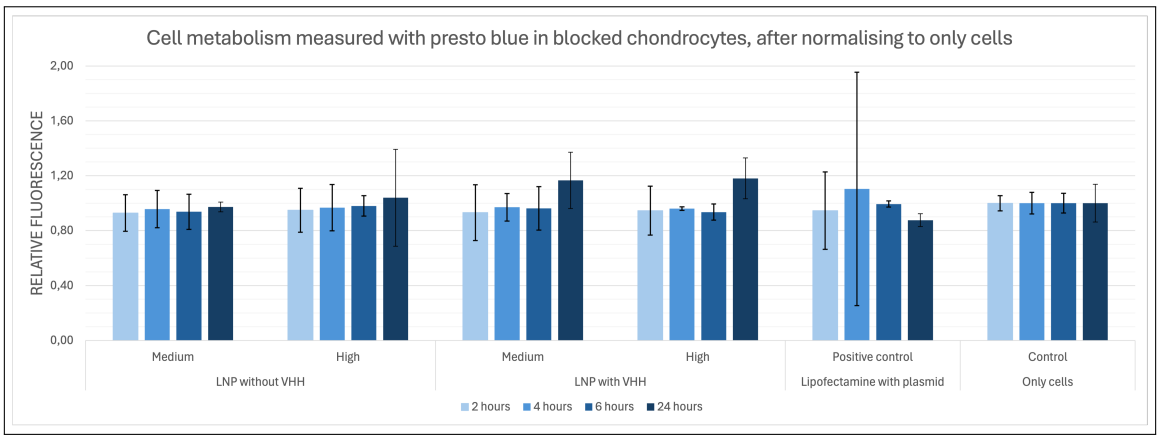

Figure 15: *Cell metabolism results measured with presto blue in blocked chondrocytes (SW1353) at four different time points (2, 4, 6 and 24 hours). Normalized to control with only cells.*

4.3 Cellular uptake and transfection

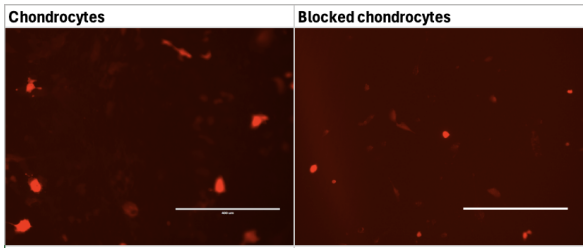

Figure 16: *Positive control with lipofectamine in both non blocked and blocked chondrocytes, assesed after 24 hours*

The positive control, consisting of cells with lipofectamine, gave a strong signal in almost all cases. For the early time points, their was no or no strong signal, but at a later time point the signal did appear, indicating that transfection had occurred. In figure 16 the pictures of the positive control can be seen. Only the macrophages showed no signal. The negative control, consisting of cells with only plasmid, gave no signal, indicating that transfection had not occurred.

4.3.1 Phase contrast microscopy

At multiple times during the experiments, the morphology of the cells has been assessed. Before adding the LNPs, the cells generally looked good. The chondrocytes were streched out and the macrophages were spherical and some of them were elongated. After adding the LNPs, there were no significant changes to the cell morphology for both cell lines. After 96 hours, more apoptotic cells were visible. The positive control, with lipofectamine, showed a lot of apoptotic cells.

4.3.2 EVOS microscopy and quantification

Both morphology and cellular uptake of LNPs in the three different experiments were captured with the EVOS microscope. Also for the signals of transfection a quantification of the EVOS pictures was done to compare the different conditions. For quantification it was assumed that in each well the same amount of cells was present. These results are shown below.

4.3.2.1 Empty and mCherry LNPs in chondrocytes (SW1353)

The pictures of the first experiment with chondrocytes are shown in figure 17. The magenta signal shows the signal with which the LNPs are marked. The red signal shows the signal of mCherry, which represents transfection in the cells.

On top the pictures of the cells washed after four hours are shown. For the high and medium concentration a signal is visible, for the low concentration no signal is visible. Also mCherry is not visible after four hours. After 24 and 96 hours, mCherry signal does show up, so transfection has occured. The mCherry signal also increased over time.

In the middle pictures of the cells washed after 24 hours are shown. For all concentrations a signal for Cy5.5 is visible. The signal was stronger for the high concentration then for the low concentration. Also, mCherry was directly visible, and this signal increased over time.

The bottom shows the results of the cells washed after 96 hours. In this case there was signal for the high en medium concentration, but not for the low concentration. Also, mCherry gives a signal which means transfection has occurred.

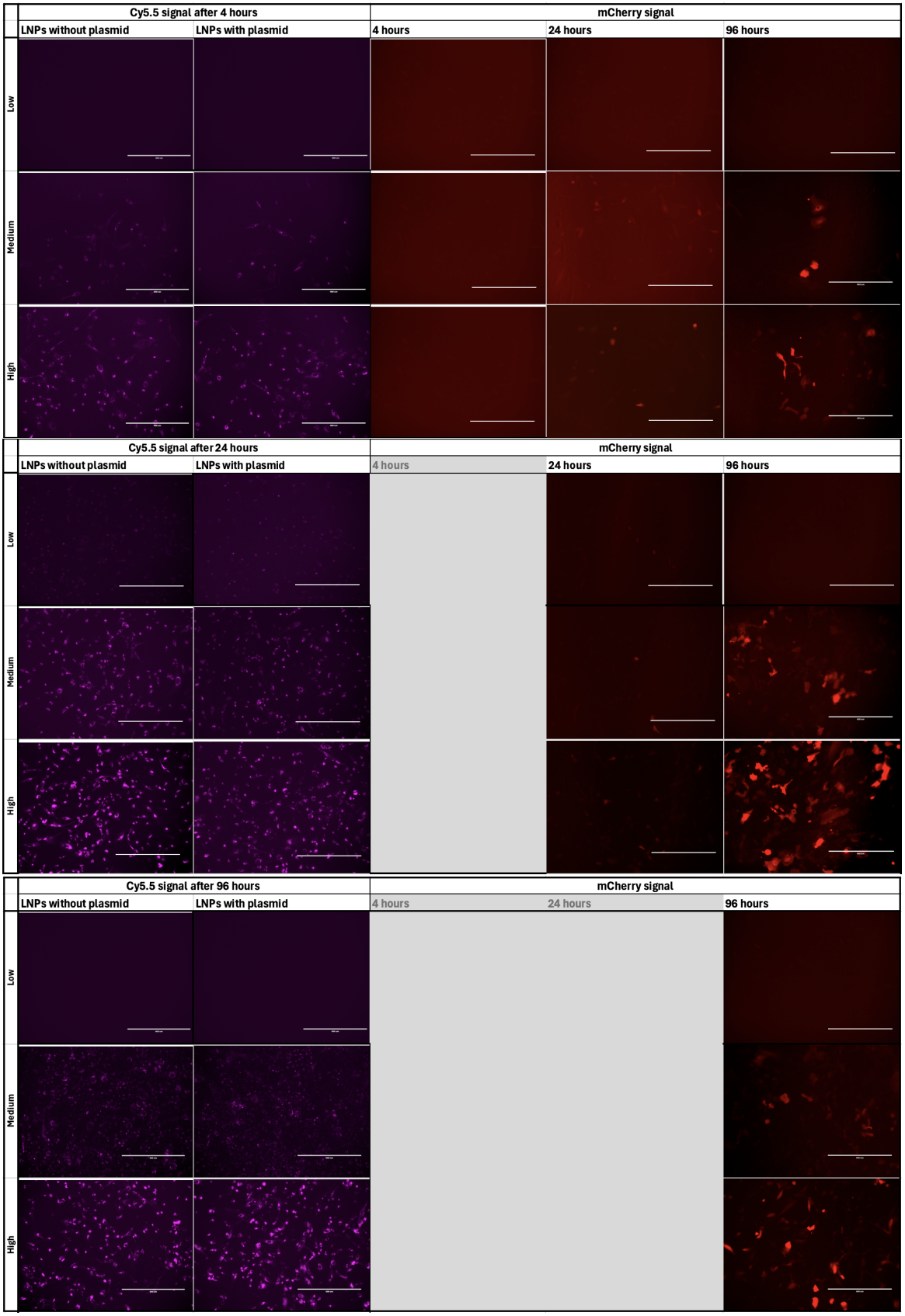

Figure 17: *Results measured with EVOS microscope of chondrocytes washed and viewed at three different time points. Magenta (on the left) shows the Cy5.5 signal with which the LNPs are marked. The red signal (on the right) shows the mCherry signal, which represent for transfection by the plasmid mCherry. The top shows the results of the cells washed 4 hours after adding the LNPs and viewed at 4, 24 and 96 hours. The middle, the results of the cells washed 24 hours after adding the LNPs and viewed at 24 and 96 hours. And the bottom the results of the cells washed 96 hours after adding the LNPs and viewed at 96 hours.*

The uptake quantification results of pictures above are shown in figure 18. For both empty and mCherry LNPs it is clearly shown, that a higher concentration of LNPs lead to a higher signal of Cy5.5. This means that more cellular uptake has taken place. For the high concentration a clear trend can be seen, that shows a higher signal over time.

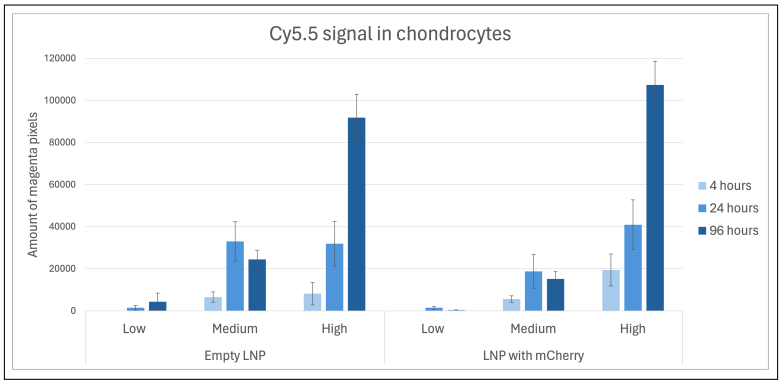

Figure 18: *Cy5.5 signal of the empty and mCherry LNPs in chondrocytes (SW1353), after 4, 24 and 96 hours*

In figure 19 the results of the mCherry signal in chondrocytes is shown. On top left the results of cells washed after four hours can be seen. The signal became stronger over time for all conditions. Also the high concentrations of LNPs gave a stronger signal than the low concentrations.
On top right the results of the cells washed after 24 hours can be seen. These results show the same trend. Higher concentration gives stronger signal and the signal increases over time.
At the bottom, the signals of the cells washed after 96 hours can be seen. Also here, a higher concentration of LNPs leads to a stronger signal.
The cells washed after 24 hours and viewed after 96 hours gave the strongest signal.

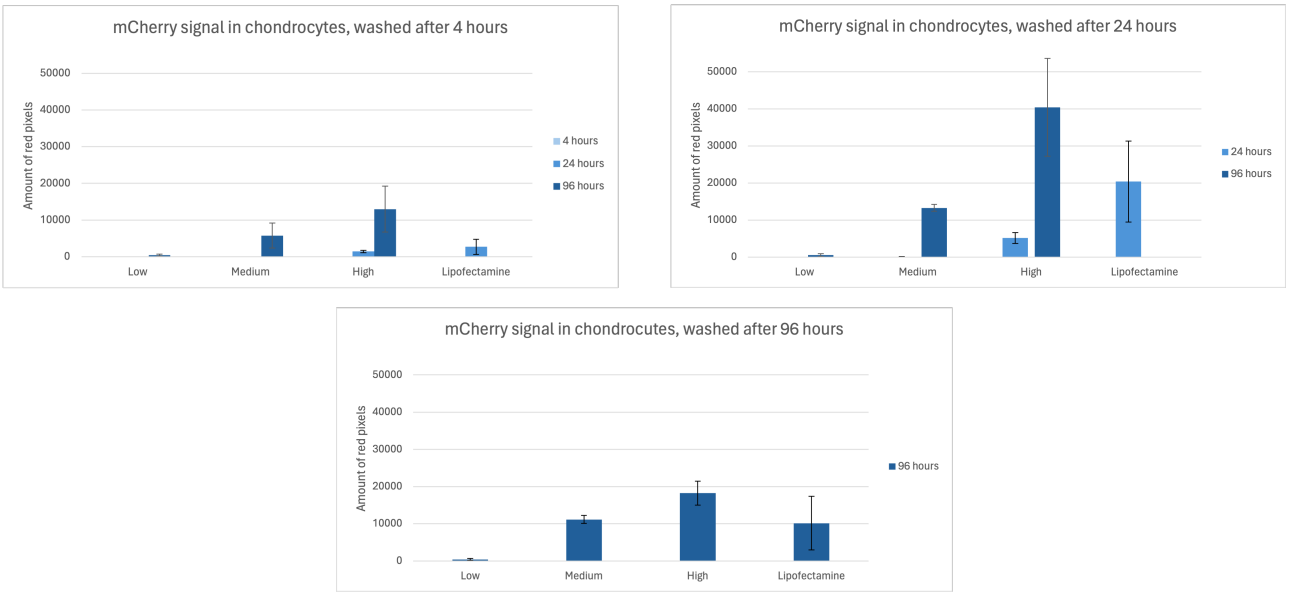

Figure 19: *mCherry signal in blocked chondrocytes (SW1353) with mCherry LNPs with and without VHH. Measured at four time points (2, 4, 6 and 24 hours).*

4.3.2.2 tRNA and mCherry LNPs in macrophages (THP-1)

The pictures of the second experiment with macrophages are shown in figure 20. The magenta signal shows again the signal with which the LNPs are marked. The red signal shows again the signal of mCherry, which represents transfection in the cells.
For all the time points and also for the control with lipofectamine, no signal of mCherry was visible.
On the left the cells washed after four hours are shown. Their was a signal visible, but a weak one. Also after 24 hours, in the middle, the signal was weak. After 96 hours, the signal was quite stronger, but still much weaker than the signals in the chondrocytes.

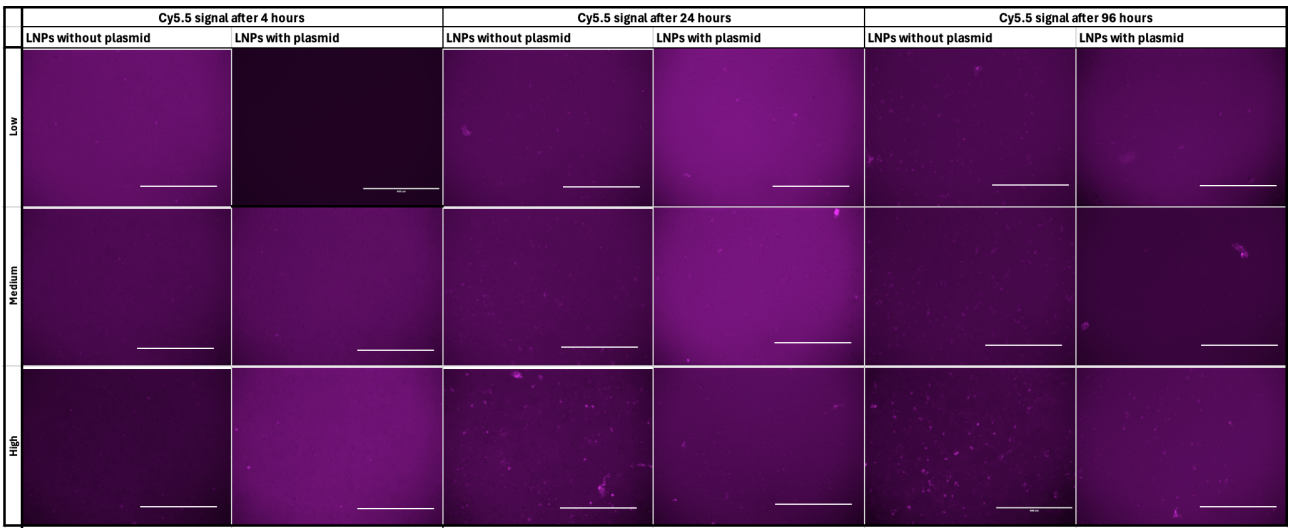

Figure 20: *Results measured with EVOS microscope of macrophages washed and viewed at three different time points. Magenta (on the left) shows the Cy5.5 signal with which the LNPs are marked. The mCherry signal was not visible. The left shows the results of the cells washed 4 hours after adding the LNPs and viewed at 4, 24 and 96 hours. The middle, the results of the cells washed 24 hours after adding the LNPs and viewed at 24 and 96 hours. And the right the results of the cells washed 96 hours after adding the LNPs and viewed at 96 hours.*

For the pictures above, the quantification results are shown in figure 21. A trend can be seen for the LNPs with tRNA, with higher concentration leading to higher Cy5.5 signal, except for the low concentration at 96 hours. This trend can also be seen for the mCherry LNPs, except for the medium concentration at 96 hours. In this experiment no signal could be seen from mCherry, it can be assumed that no translation took place.

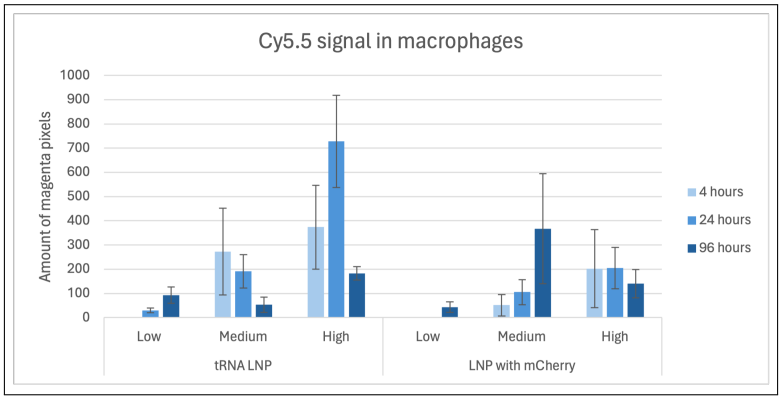

Figure 21: *Cy5.5 signal of the tRNA and mCherry LNPs in macrophages (THP-1), after 4, 24 and 96 hours*

4.3.2.3 mCherry LNPs with and without VHH in chondrocytes (SW1353)

In figure 22 the results of the mCherry signal in both blocked and non blocked chondrocytes is shown. These cells are assessed after 2, 4, 6 and 24 hours. The figures show only the mCherry pictures of the LNPs without VHH, because the LNPs with VHH did not give a signal anywhere.

The cells washed after 2 hours gave no signal. For the cells washed after 4 hours, weak signal of the LNPs was seen for the high concentration of non blocked cells and both concentrations of the blocked cells, as shown in the figure on top. Also transfection occurred in the non blocked chondrocytes with a high concentration of LNPs, because a signal was seen after 24 hours.

In the middle the cells washed after 6 hours can be seen. Here a weak signal can be seen for almost all concentrations, only for the low concentration of the LNPs with VHH not. Transfection has also taken place in these cells, as a weak signal of this can be seen after 24 hours.

At the bottom the cells washed after 24 hours are shown. Here also a weak signal can be seen for almost all concentrations, only for the low concentration of the LNPs with VHH not. And for transfection the same also applies as for the cells washed after 6 hours: transfection has occurred, because after 24 hours a weak signal is seen.

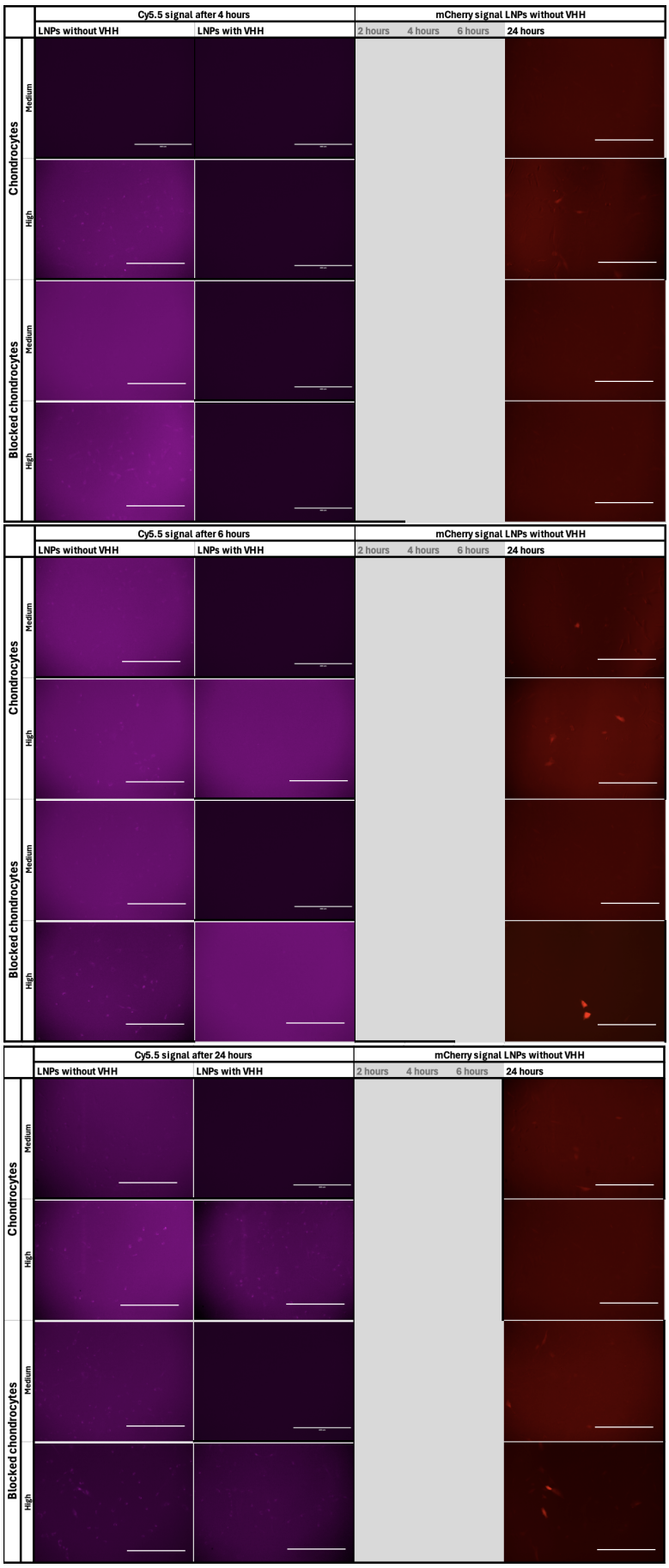

Figure 22: *Results measured with EVOS microscope of blocked and non blocked chondrocytes washed and viewed at four different time points. Magenta (on the left) shows the Cy5.5 signal with which the LNPs are marked. The red signal (on the right) shows the mCherry signal, which represent for transfection by the plasmid mCherry. The figures show only the mCherry pictures of the LNPs without VHH, because the LNPs with VHH did not give a signal anywhere. The top shows the results of the cells washed 4 hours after adding the LNPs and viewed at 4, 6 and 24 hours. The middle, the results of the cells washed 6 hours after adding the LNPs and viewed at 6 and 24 hours. And the bottom the results of the cells washed 24 hours after adding the LNPs and viewed at 24 hours.*

In the figures below, figure 23 and figure 24, the results of the experiments with LNPs with and without VHH are shown, with non blocked cells in figure 23 and blocked cells in 24. The non blocked cells show a higher uptake for the high concentration of LNPs, for both the LNPs with and without VHH. For the LNPs without VHH the high concentration gave a stronger signal after 24 hours, than after 96 hours.
The blocked cells show the same trend, high concentration gave a stronger signal. In this case, the uptake increases over time for all conditions.

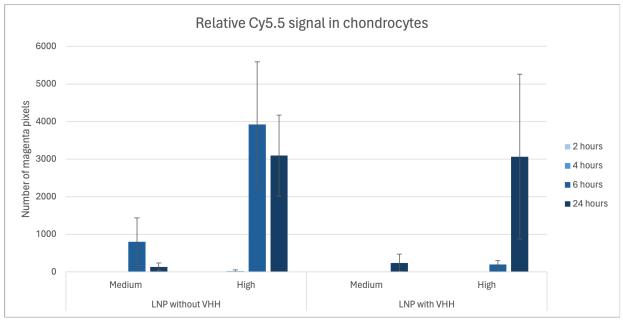

Figure 23: *Cy5.5 signal of the mCherry LNPs with and without VHH in chondrocytes (SW1353), after 2, 4, 6 and 24 hours*

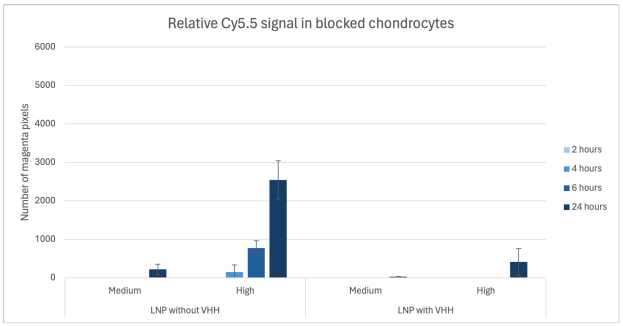

Figure 24: *Cy5.5 signal of the mCherry LNPs with and without VHH in chondrocytes (SW1353) blocked with loose VHH, after 2, 4, 6 and 24 hours*

For non blocked cells, the results of the quantification are shown in figure 25. For the cells washed after two hours, no signal was seen, also not at a later time point. For cells washed after four hours, no signal could be seen immediately. After 24 hours a weak signal was visible for the medium concentration without VHH. For the cells washed after six hours, no signal could be seen immediately. But after 24 hours a signal was visible for both concentrations of LNPs without VHH. For cells washed after 24 hours, a signal can be seen directly for the LNPs without VHH.
For the blocked cells, the results of the quantification are shown in figure 26. For the cells washed after two hours, no signal can be seen, also not at a later time point. For the cells washed after four hours only a weak signal can be seen after 24 hours for the high concentration LNPs without VHH. For the cells washed after six hours only a signal can be seen after 24 hours for the high concentration LNPs without VHH. For the cells washed after 24 hours a weak signal can be seen for the LNPs without VHH.

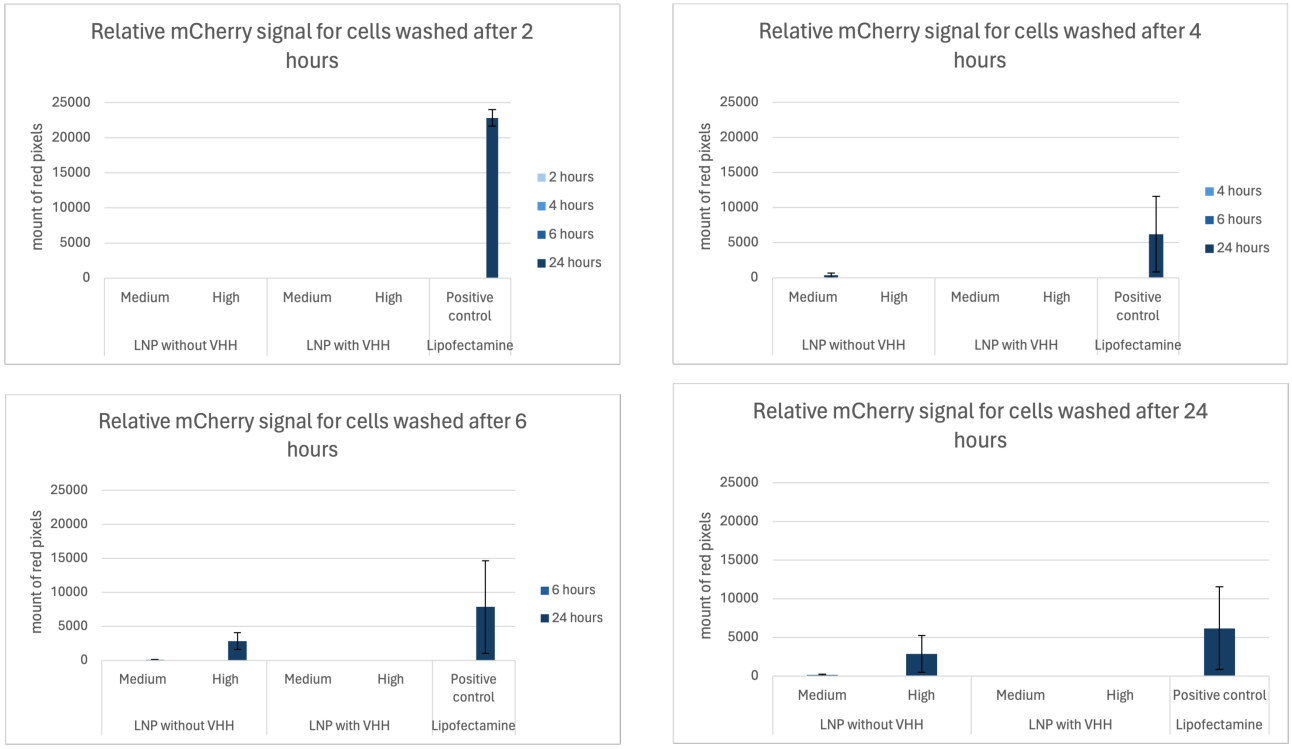

Figure 25: *mCherry signal in chondrocytes (SW1353) with mCherry LNPs with and without VHH. Measured at four time points (2, 4, 6 and 24 hours).*

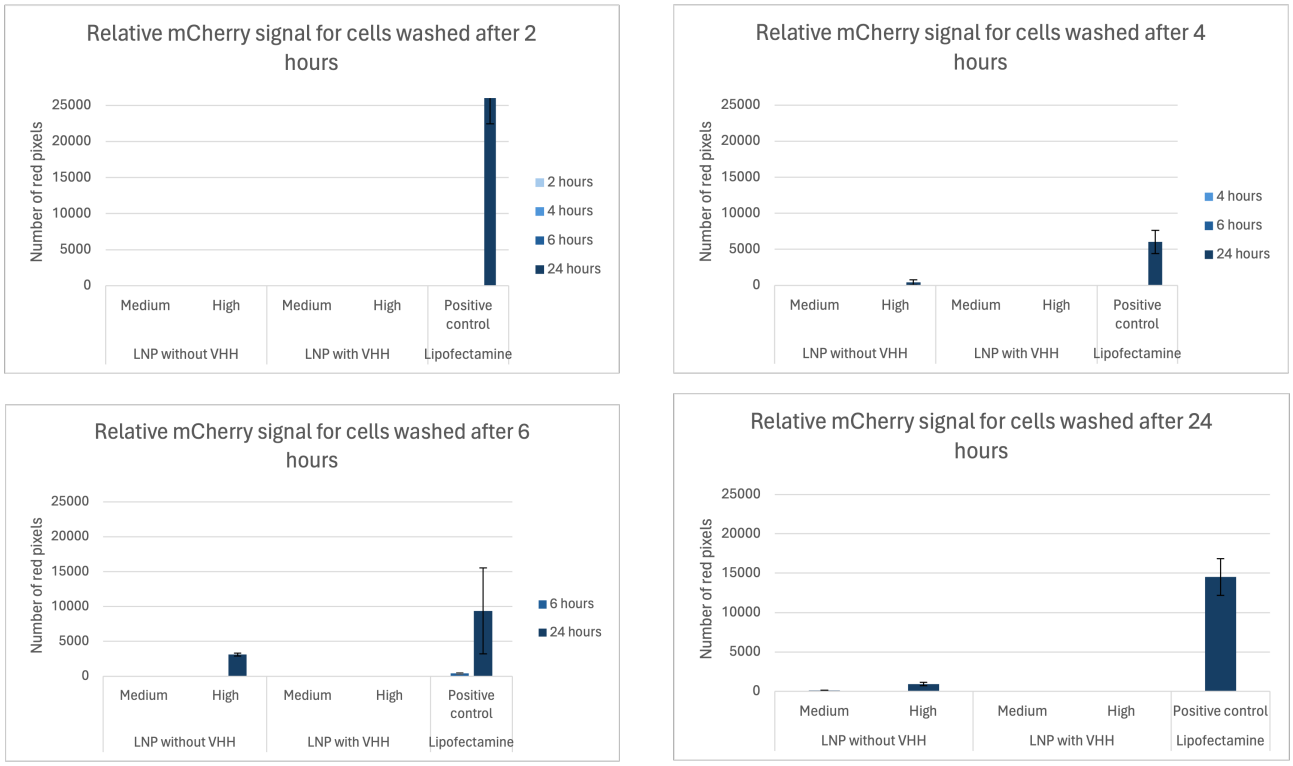

Figure 26: *mCherry signal in blocked chondrocytes (SW1353) with mCherry LNPs with and without VHH. Measured at four time points (2, 4, 6 and 24 hours).*

5 Discussion and conclusion

The yield of nanoparticle fabrication was good. Only for the LNPs with mCherry inside a new batch needed to be made. A larger batch would be better, because this makes it easier to compare the different concentrations. The size of the LNPs was also good and as expected. Only the tRNA LNPs were bigger and had a higher PDI, which means they are less stable. A reason could be that this is the first type of LNP made during this experiment. These LNPs were used for the experiment with macrophages. These results gave a lower uptake of LNPs than the results of chondrocytes. The lower stability of LNPs could be a reason, but also the mCherry LNPs gave a lower uptake and these had a low PDI.

The DNA assay was not as expected and it is questionable if the results are valid. The stock concentration of mCherry was 0.14ug/ul, but if the results of the DNA assay were followed the concentration would be 0.005ug/ul.
For this experiment, the LNPs were degraded with trisol. The degraded LNPs were measured, while in trisol and after being centrifuged and dissolved in PBS. The first measurement gave a much lower concentration than the second measurement, which shows that trisol affects the measurement. For the second experiment, the degraded LNPs still gave a lower signal than the complete LNPs. Even if there is a lot of DNA on the outside of the LNP, the degraded LNPs should have a higher or the same concentration. For next experiments, something else should be used to degrade the LNPs or the degraded LNPs should be washed, to remove all the trisol.

The coupling of the lipid to VHH was succesfull. However, the yield of the coupling was not very high. In fact, the band at 15kDa is thicker than the band at 25kDa. Which means, there is more loose VHH than coupled lipid-VHH.

The SPR data shows that the human receptor interacted with both the loose VHH and the lipid-VHH. Additionally, it shows that this is a specific interaction, because the canine and equine receptors did not give a clear signal.
The signal of the lipid-VHH was lower than the signal of the loose VHH, possibly caused by a low efficiency of the coupling.

As described in the results, the experiment with empty and mCherry LNPs with chondrocytes shows a lower metabolic activity for a higher concentration of both types of LNPs. Specific for the LNPs with mCherry inside a decreasing metabolic activity can be seen over time and with a higher concentration. This shows that the LNPs are slightly toxic to the cells. And because of the decreasing metabolic activity over time, it can be said that transfection with mCherry is more toxic to the cells than the LNPs by themselves.
It may also be that the LNPs with mCherry inside have different properties than the empty LNPs, leading to lower metabolic activity. Surface charge could be an example. Cationic NPs are more toxic to cells than anionic NPs [24]. Going forward, this could be measured with Zeta potential.
After 96 hours the metabolic activity seems to increase for both the medium and low concentration, this may indicate that the cells are recovering over time.

The LNPs seem to be as toxic for the macrophages as for the chondrocytes. After four and 24 hours, the metabolic activity is about the same as for the control with only cells. After 96 hours a lower metabolic activity of around 0.7 can be seen. This is also the case for chondrocytes. For the macrophages there is not a big difference between the LNPs either with and without mCherry. A explanation can be that macrophages are difficult to transfect, so mCherry does not reach the nucleus and is therefore less toxic [25].

The condition with non blocked chondrocytes to which LNPs without VHH were added is the same as the condition in the first experiment. However, they do not show the same results. In the first experiment, the metabolic activity is slightly lower after 24 hours than after four hours. But in the last experiment, the metabolic activity is same after 24 hours than after four hours. Overall, cell metabolism is lower in the latter experiment, around 7000, than in the former, around 9000, as shown in appendix B. This difference could be caused by a higher passage number of the last experiment. A higher passage number may lead to reduced proliferation, which is aligned with lower metabolic activity [26].
For the cells to which LNPs with VHH are added, the metabolic activity becomes higher over time, even higher than the control with just cells. Higher metabolic activity can be caused by many different factors. Factors such as environmental factors and amount of cells are similar in all conditions, so that will not be a cause. However, the membrane potential could be an option. The membrane potential is slightly negative in rest, when becoming less negative, an action potential is created, causing faster uptake of the intracellular conversion of presto blue. For the cells measured after 24 hours, LNPs are present in and on the cells. Binding of the VHH on the surface of the cells can lead to a less negative membrane potential, if the VHH LNPs are slightly positive [27].

However, these are only assumptions. To prove this, zeta potential should be measured in subsequent experiments of the LNPs with and without VHH.

For the blocked cells, the trend seems to be the same, negating this reason. Unless cell blocking is unsuccessful, which stops specific uptake. To test if the blocking was successful, the individual VHHs would also have to be stained.
There is a possibility cell blocking was successful, because cell blocking does not prevent nonspecific uptake. With non specific uptake the LNPs are also present on the surface of the cell, so the surface charge also changes, which will still result in a higher metabolic activity.

Quantification of the EVOS figures was done by determining the number of red/magenta pixels in the EVOS images. Here it was assumed that there is approximately the same number of cells in each well and thus in each picture. This was not true in all cases, making the results questionable. In the future, the number of pixels per cell should be determined to get a more reliable result and to compare the results. Determining the number of cells in the picture can be done with the EVOS microscope. For this, the cells must be stained with DAPI beforehand.

The cellular uptake in the chondrocytes is as expected. As shown in the results, a higher concentration of LNPs leads to a stronger signal which increases over time.
An unexpected thing is that medium concentration shows the highest signal after 24 hours instead of after 96 hours. These conditions shows a lower metabolic activity than after 96 hours. Cells have a feedback mechanism that can ensure feedback when too much uptake leads to toxicity. In cells where a medium concentration of LNPs is added, this mechanism can be triggered over time. In doing so, uptake is inhibited. This can lead to less uptake after 96 hours than after 24 hours [28]. For the high concentration this can also occur, but because the concentration of LNPs there is so high the uptake remains the same.

The trend seen in the uptake in macrophages is also as expected, except for the high concentration after 96 hours for both types of LNPs and the medium concentration for the tRNA LNPs. This uptake is lower than expected. Possibly after 96 hours a lot of cells are dead and washed away. It is also known that apoptotic cells are more permeable, therefore it could mean that during the washing steps the LNPs were washed out of the cells [29].
If the results are compared with those of chondrocytes, the uptake is much lower, about one hunderd times. Macrophages are difficult cells to culture. They have special requirements and are quick not to be cheerful if something is not to their liking. In this experiment, macrophages were treated with LPS to let them sink down on the bottom and differentiate. However, LPS does not appear to work for differentiation. LPS causes the cytokines of macrophages to be activated. For the macrophages to differentiate, PMA will have to be used [30]. The lower uptake of LNPs by the macrophages might be because the macrophages were not treated with PMA and thus not differentiated.

For the cells to which LNPs with and without VHH are added, the signals are a bit weaker than in the first experiment, while one condition (chondrocytes with mCherry LNPs) is the same. The only difference between the two experiments is the passage number of the cells. In the former experiment the cells had a lower passage number, than in the latter experiment. A higher passage number lead to lower metabolic activity and this can also affect the uptake mechanism [26]. Going forward, this experiment should be performed with chondrocytes with a low passage number, around 4.
Also, for the non blocked cells, the signal after four hours is stronger than after 24 hours. This may have the same cause as in the first experiment with chondrocytes, looking at the feedback mechanism of cells. Whereby longer exposure to LNPs leads to excessive uptake, which becomes toxic and inhibits uptake [28].
As shown in the results, the LNPs without VHH gave a higher uptake than the LNPs with VHH. This is not as expected, because it was thought the VHH would lead to better and more uptake. The uptake of LNPs can be affected by many conditions. As previously mentioned by surface charge, but also by size, shape and hydrophobicity. In this study, surface charge was not determined. This should be done for follow-up studies. The size of the LNPs was determined and the VHH makes no difference, both LNPs are about the same size. The shape of the LNPs has also not been determined in this study for both of the LNPs with and without the VHH. This could be investigated in the future, for example with Cryo Transmission Electron Microscopy (cryo-TEM) [31].
Finally, hydrophobicity may influence the uptake of LNPs. Cells have a hydrophilic outer membrane and will therefore interact better with hydrophilic particles. The LNPs all have PEGylation on the surface, so this would expect them to be well absorbed [32]. In the case of the LNPs with VHH, there is VHH bound to the PEG chain. It could be that this VHH is hydrophobic, reducing absorption.
Additionally, thoughts beforehand were that the VHH would bind to the outside of the cells and then be absorbed

at a later time. This cannot be seen in the EVOS pictures. This makes it questionable whether the LNPs with VHH were taken up by binding to the receptor or whether they were taken up via phagocytosis.
The blocked cells result in a lower signal for the LNPs with VHH, which means less uptake, compared to the non blocked cells. In the blocked cells, the IR-1L1 receptors are occupied, therefore the LNPs with VHH can no longer bind to them and no specific uptake will occur. The uptake that can still be seen in the blocked cells may be nonspecific uptake, for example due to phagocytosis. In the non blocked cells, both specific and nonspecific uptake can occur, which may lead to a higher uptake.

The results of the transfection experiment with chondrocytes with empty and mCherry LNPs are as expected. The cells that are washed after four hours show that the signal increases over time and that a higher concentration gives a stronger signal. After 24 and 96 hours this same trend can be seen. For the next time, also the positive control need to be assessed at all time points and not only at the first time point directly after washing the cells.
To compare the results with the lipofectamine control, the concentration of mCherry used with lipofectamine should be the same as for the LNPs.

The THP-1 cells did not show transfection. Also the positive control with lipofectamine, did not show any signal. Afterwards, this was as expected, because macrophages are difficult cells to transfect, as mentioned before [25].

For the non blocked cells, there was either no or a really weak signal at 2 and 4 hours. This is as expected, because transfection did not occur this fast. After 24 hours, the signal is still low. For the next time, maybe a measurement should be done at 96 hours, because even for the earlier experiments, not much transfection was seen after 4 and 24 hours. Also the control with lipofectamine at most conditions gave a signal only after 24 hours, so it is not directly due to the LNPs.
For the blocked cells the same trend can be seen as for the non blocked cells. The only difference is that the mCherry signals was not visible. One reason for this may be that there was less LNP uptake in the blocked cells, resulting in less mCherry present in these cells.

The research question of this study was: **What is the influence of targeting with VHHs on the uptake of LNPs and transfection in joint cells?**
In conclusion, the LNPs have a small diameter in the nm scale and have almost all about the same diameter. The PDI of almost all of the LNPs is low, which means they are stable. It cannot be said with certainty whether mCherry is present on the inside or the outside of the LNPs. The coupling between lipid and VHH was successful, but the efficiency was low. Both the loose VHH and de lipid VHH bind to the human IR-1L1 receptor.
When looking at the metabolic activity, both chondrocytes and macrophages show the same metabolic activity. After four and 24 hours, the metabolic activity did not differ much from the control with only cells, but after 96 hours, metabolic activity becomes lower. For chondrocytes, transfection leads to even lower metabolic activity. LNPs with VHH give a higher metabolic activity.
The cellular uptake of LNPs without VHH is higher in chondrocytes than in macrophages. Also, a higher concentration of LNPs leads to a about $\sim$ten times higher cellular uptake. When VHH is added to the LNPs the cellular uptake in chondrocytes is less.
Transfection occured in chondrocytes but not in macrophages. Again, the trend can be seen that a higher concentration of LNPs leads to a higher signal for transfection, about $\sim$two times. LNPs with VHH do not lead to transfection.
Concluding that VHHs do have an influence on the uptake of LNPs in joint cells, but in the opposite as expected. So, the proof of concept did not succeed. But this does not rule out the possibility that there may not be a positive effect on cellular uptake, as further research needs to be done.

Future research could look at multiple of things.
First, in this study the quantification of the cellular uptake is done with Matlab, for next experiments flow cytometry in combination with EVOS microscopy would be a better choice. This would allow all cells from the well to be included in the measurement [33]. EVOS microscopy can still be used to look at the intensity of the signals, the morphology of the cells and possibly the location of the LNPs.
Secondly, in order to see if the LNPs with VHH bind to the receptor first and only then are absorbed, a time lapse with EVOS could be made. Here the LNPs can be followed by the staining.
Thirdly, their should be looked at why LNPs with VHH cause reduced uptake compared to LNPs without VHH, since this goes against expectations. Subjects that can be looked into are, as mentioned before, the surface charge of the LNPs. Also the shape of the LNPs can be looked at with cryo-TEM. Finally, hydrophilicity of the

VHHs would also be an interesting subject to look at.
Lastly, the future aim is to deliver drugs with the LNPs to specific cells. In this study the loaded LNPs (with plasmid) seem to be more toxic to the cells than the non loaded LNPs. Follow-up studies should look into the toxicity of miRNA when inside the LNPs.

A Appendix 1

```

[row, column, ~] = size(picture);
redchannel = picture(:,:,1);
red_lowerlimit = 90;
red_upperlimit = 254;
amount_red_pixels = 0;

for i = 1:row
    for j = 1:column
        pixel = double(redchannel(i, j));
        if pixel >= red_lowerlimit & pixel <= red_upperlimit
                amount_red_pixels = amount_red_pixels + 1;
                picture_red(i,j) = pixel;
        else
            picture_red(i,j) =0;
        end
    end
end
imshow(picture_red,[])
disp(['Amount of red pixels in the picture: ', num2str(amount_red_pixels)]);
```

B Appendix 2

The results of the cell metabolism measurement are shown below, before normalizing.

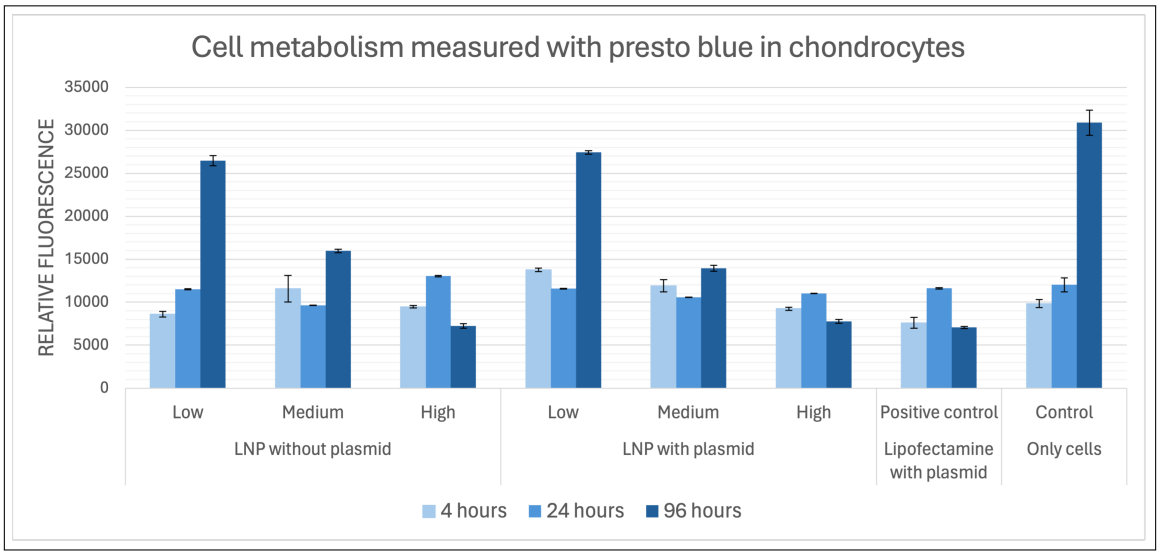

Figure 27: *Cell metabolism results measured with presto blue in chondrocytes with empty and mCherry LNPs, at three different time points (4, 24 and 96 hours) in a dilution series of 4-40-400x.*

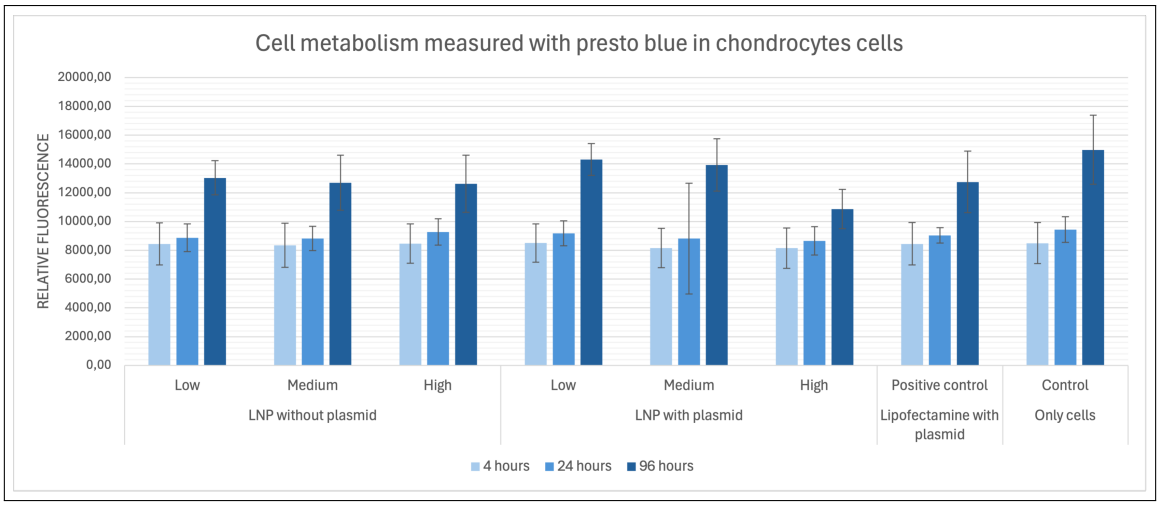

Figure 28: *Cell metabolism results measured with presto blue in chondrocytes with empty and mCherry LNPs, at three different time points (4, 24 and 96 hours) in a dilution series of 40-400-4000x.*

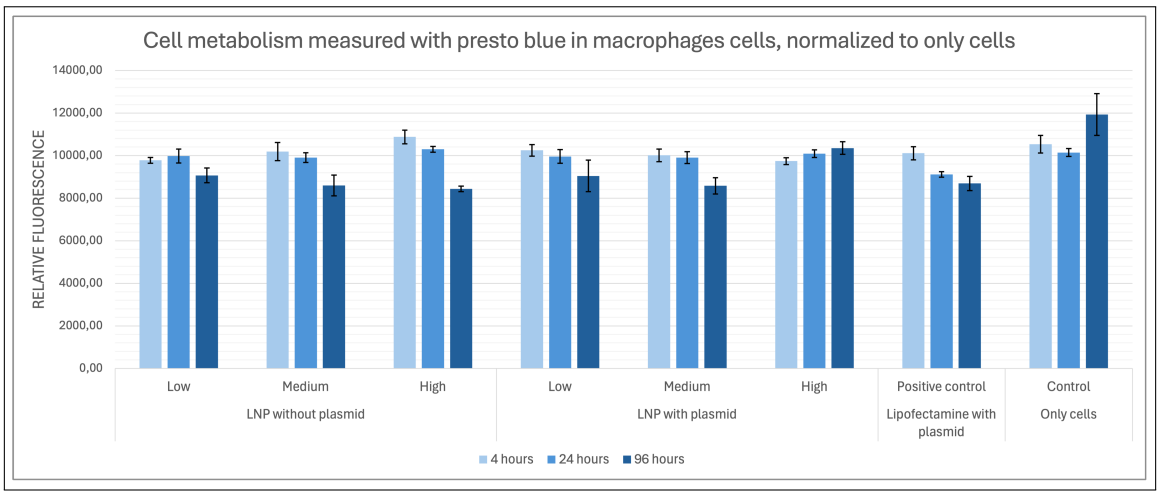

Figure 29: *Cell metabolism results measured with presto blue in macrophages with tRNA and mCherry LNPs, at three different time points (4, 24 and 96 hours) in a dilution series of 40-400-4000x.*

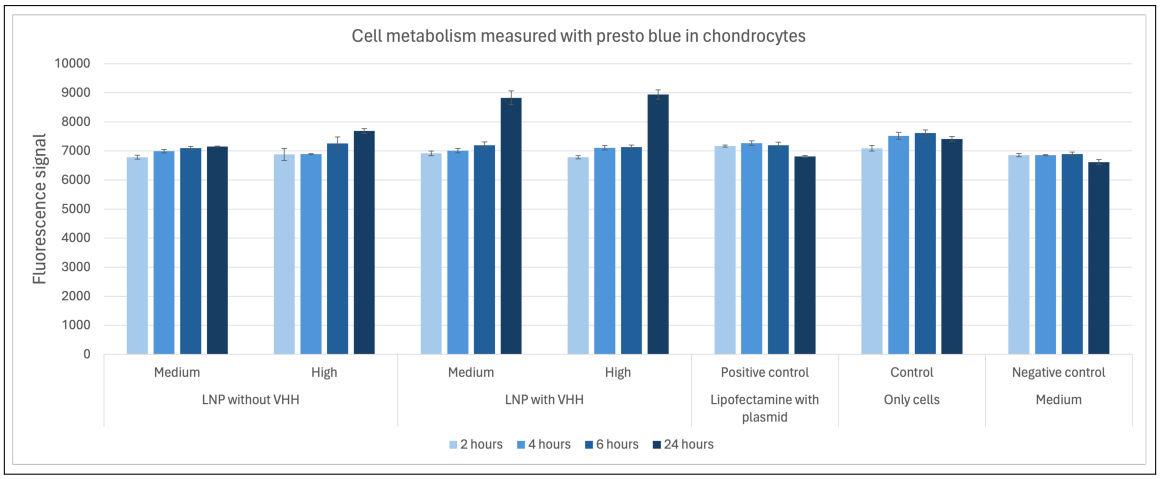

Figure 30: *Cell metabolism results measured with presto blue in chondrocytes with mCherry LNPs with and without VHH, at three different time points (4, 24 and 96 hours) in a dilution series of 40-400-4000x. The values are normalized to the control with only cells.*

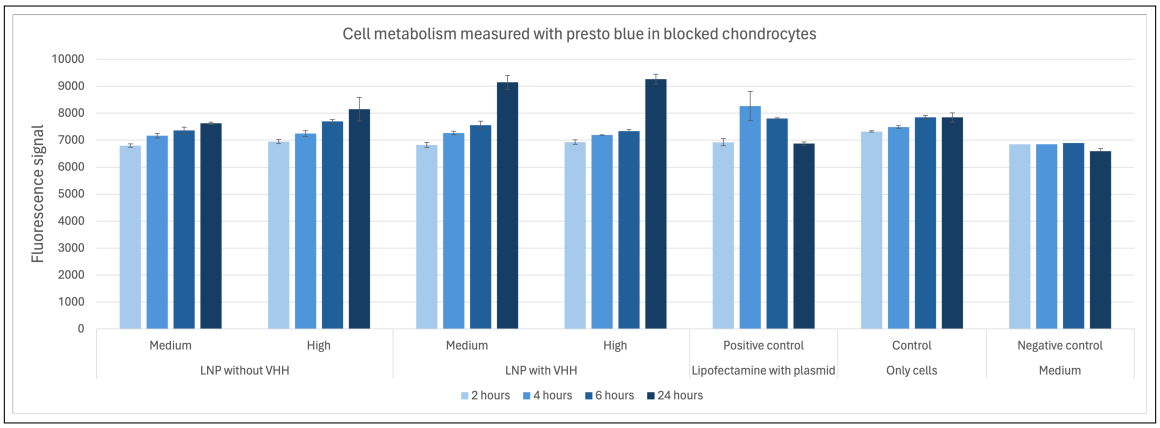

Figure 31: *Cell metabolism results measured with presto blue in blocked chondrocytes with mCherry LNPs with and without VHH, at three different time points (4, 24 and 96 hours) in a dilution series of 40-400-4000x. The values are normalized to the control with only cells.*

References

[1] Geng R, Li J, Yu C, Zhang C, Chen F, Chen J, et al. Knee osteoarthritis: Current status and research progress in treatment (Review). Experimental and therapeutic medicine. 2023 8;26(4). Available from: https://pubmed.ncbi.nlm.nih.gov/37745043/. doi:10.3892/ETM.2023.12180.

[2] Mathiessen A, Conaghan PG. Synovitis in osteoarthritis: Current understanding with therapeutic implications. Arthritis Research and Therapy. 2017 2;19(1):1–9. Available from: https://arthritis-research.biomedcentral.com/articles/10.1186/s13075-017-1229-9. doi:10.1186/S13075-017-1229-9/FIGURES/2.

[3] White CM, Kesler WW, Miner L, Flemming D. MR Imaging Knee Synovitis and Synovial Pathology. Magnetic resonance imaging clinics of North America. 2022 5;30(2):277–291. Available from: https://pubmed.ncbi.nlm.nih.gov/35512890/. doi:10.1016/J.MRIC.2021.11.007.

[4] Scanzello CR, Goldring SR. The role of synovitis in osteoarthritis pathogenesis. Bone. 2012 8;51(2):249–257. Available from: https://pubmed.ncbi.nlm.nih.gov/22387238/. doi:10.1016/J.BONE.2012.02.012.

[5] Sharma L. Osteoarthritis of the Knee. New England Journal of Medicine. 2021 1;384(1):51–59. Available from: https://www.nejm.org/doi/full/10.1056/NEJMcp1903768. doi:10.1056/NEJMCP1903768.

[6] Wu Y Z X A CL, Harasymowicz Y Z X A NS, Klimak Y Z X K MA, Collins Y Z X KH, Guilak Y Z X F. The role of macrophages in osteoarthritis and cartilage repair. 2020. Available from: https://-doi.org/10.1016/j.joca.2019.12.007. doi:10.1016/j.joca.2019.12.007.

[7] Cutolo M, Campitiello R, Gotelli E, Soldano S. The Role of M1/M2 Macrophage Polarization in Rheumatoid Arthritis Synovitis. Available from: www.frontiersin.org. doi:10.3389/fimmu.2022.867260.

[8] Hu J, Huang S, Liu X, Zhang Y, Wei S, Hu X. miR-155: An Important Role in Inflammation Response. Journal of Immunology Research. 2022;2022. Available from: /pmc/articles/PMC9007653/ /pmc/articles/PMC9007653/?report=abstract https://www.ncbi.nlm.nih.gov/pmc/articles/PMC9007653/. doi:10.1155/2022/7437281.

[9] Jia H, Chen H, Wei M, Chen X, Zhang Y, Cao L, et al. Gold nanoparticle-based miR155 antagonist macrophage delivery restores the cardiac function in ovariectomized diabetic mouse model. International Journal of Nanomedicine. 2017 7;12:4963–4979. doi:10.2147/IJN.S138400.

[10] Kang M, Huang CC, Lu Y, Shirazi S, Gajendrareddy P, Ravindran S, et al. Bone regeneration is mediated by macrophage extracellular vesicles. 2020. Available from: https://doi.org/10.1016/j.bone.2020.115627. doi:10.1016/j.bone.2020.115627.

[11] Essandoh K, Li Y, Huo J, Fan GC. MiRNA-Mediated Macrophage Polarization and Its Potential Role in the Regulation of Inflammatory Response. Shock (Augusta, Ga). 2016 8;46(2):122. Available from: /pmc/articles/PMC4949115/ /pmc/articles/PMC4949115/?report=abstract https://www.ncbi.nlm.nih.gov/pmc/articles/PMC4949115/. doi:10.1097/SHK.0000000000000604.

[12] Moradian H, Roch T, Lendlein A, Gossen M. mRnA transfection-induced Activation of primary Human Monocytes and Macrophages: Dependence on carrier System and Nucleotide Modification. Available from: https://doi.org/10.1038/s41598-020-60506-4. doi:10.1038/s41598-020-60506-4.

[13] Zong Y, Lin Y, Wei T, Cheng Q. Lipid Nanoparticle (LNP) Enables mRNA Delivery for Cancer Therapy. Advanced Materials. 2023 12;35(51):2303261. Available from: https://onlinelibrary.wiley.com/-doi/full/10.1002/adma.202303261 https://onlinelibrary.wiley.com/doi/abs/10.1002/adma.202303261 https://onlinelibrary.wiley.com/doi/10.1002/adma.202303261. doi:10.1002/ADMA.202303261.

[14] Jung HN, Lee SY, Lee S, Youn H, Im HJ. Lipid nanoparticles for delivery of RNA therapeutics: Current status and the role of in vivo imaging. Theranostics. 2022;12(17):7509. Available from: /pmc/articles/PMC9691360/ /pmc/articles/PMC9691360/?report=abstract https://www.ncbi.nlm.nih.gov/pmc/articles/PMC9691360/. doi:10.7150/THNO.77259.

[15] Bordon G, Berenbaum F, Distler O, Luciani P. Harnessing the multifunctionality of lipid-based drug delivery systems for the local treatment of osteoarthritis. Biomedicine & pharmacotherapy = Biomedecine & pharmacotherapie. 2023 12;168. Available from: https://pubmed.ncbi.nlm.nih.gov/37939613/. doi:10.1016/J.BIOPHA.2023.115819.

[16] Hald Albertsen C, Kulkarni JA, Witzigmann D, Lind M, Petersson K, Simonsen JB. The role of lipid components in lipid nanoparticles for vaccines and gene therapy. Advanced drug delivery reviews. 2022 9;188. Available from: https://pubmed.ncbi.nlm.nih.gov/35787388/. doi:10.1016/J.ADDR.2022.114416.

[17] Xu L, Wang X, Liu Y, Yang G, Falconer RJ, Zhao CX. Lipid Nanoparticles for Drug Delivery. Advanced NanoBiomed Research. 2022 2;2(2):2100109. Available from: https://onlinelibrary.wiley.com/doi/full/10.1002/anbr.202100109 https://onlinelibrary.wiley.com/doi/abs/10.1002/anbr.202100109 https://onlinelibrary.wiley.com/doi/10.1002/anbr.202100109. doi:10.1002/ANBR.202100109.

[18] Paunovska K, Loughrey D, Dahlman JE, Coulter WH. Drug delivery systems for RNA therapeutics. Available from: www.nature.com/nrg. doi:10.1038/s41576-021-00439-4.

[19] Behzadi S, Serpooshan V, Tao W, Hamaly MA, Alkawareek MY, Dreaden EC, et al. Cellular Uptake of Nanoparticles: Journey Inside the Cell. Chemical Society reviews. 2017 7;46(14):4218. Available from: /pmc/articles/PMC5593313/ /pmc/articles/PMC5593313/?report=abstract https://www.ncbi.nlm.nih.gov/pmc/articles/PMC5593313/. doi:10.1039/C6CS00636A.

[20] Alexis F, Rhee JW, Richie JP, Radovic-Moreno AF, Langer R, Farokhzad OC. New frontiers in nanotechnology for cancer treatment. Urologic Oncology: Seminars and Original Investigations. 2008 1;26(1):74–85. doi:10.1016/J.UROLONC.2007.03.017.

[21] Chen W, Yuan Y, Jiang X. Antibody and antibody fragments for cancer immunotherapy. Journal of controlled release : official journal of the Controlled Release Society. 2020 12;328:395–406. Available from: https://pubmed.ncbi.nlm.nih.gov/32853733/. doi:10.1016/J.JCONREL.2020.08.021.

[22] Richards DA, Maruani A, Chudasama V. Antibody fragments as nanoparticle targeting ligands: a step in the right direction. Chemical Science. 2017 1;8(1):63. Available from: /pmc/articles/PMC5304706/ /pmc/articles/PMC5304706/?report=abstract https://www.ncbi.nlm.nih.gov/pmc/articles/PMC5304706/. doi:10.1039/C6SC02403C.

[23] Xu J, Xu K, Jung S, Conte A, Lieberman J, Muecksch F, et al. Nanobodies from camelid mice and llamas neutralize SARS-CoV-2 variants. Nature 2021 595:7866. 2021 6;595(7866):278–282. Available from: https://www.nature.com/articles/s41586-021-03676-z. doi:10.1038/s41586-021-03676-z.

[24] Fröhlich E. The role of surface charge in cellular uptake and cytotoxicity of medical nanoparticles. International journal of nanomedicine. 2012;7:5577–5591. Available from: https://pubmed.ncbi.nlm.nih.gov/23144561/. doi:10.2147/IJN.S36111.

[25] Schnoor M, Buers I, Sietmann A, Brodde MF, Hofnagel O, Robenek H, et al. Efficient non-viral transfection of THP-1 cells. Journal of immunological methods. 2009 5;344(2):109–115. Available from: https://pubmed.ncbi.nlm.nih.gov/19345690/. doi:10.1016/J.JIM.2009.03.014.

[26] Kang SW, Yoo SP, Kim BS. Effect of chondrocyte passage number on histological aspects of tissue-engineered cartilage. Bio-Medical Materials and Engineering. 2007 1;17(5):269–276.

[27] Alberts D Bruce; Bray. Transport across cell membranes . In: Essential cell biology. fourth edition ed.; 2013. p. 383–388.

[28] Krishna S, Semsey S, Sneppen K. Combinatorics of feedback in cellular uptake and metabolism of small molecules. Proceedings of the National Academy of Sciences of the United States of America. 2007 12;104(52):20815–20819. Available from: www.pnas.orgcgidoi10.1073pnas.0706231105. doi:10.1073/PNAS.0706231105/SUPPL_FILE/06231SUPPTEXT.PDF.

[29] Savitskaya MA, Onishchenko GE. Mechanisms of apoptosis. Biochemistry (Moscow). 2015 11;80(11):1393–1405. Available from: https://link.springer.com/article/10.1134/S0006297915110012. doi:10.1134/S0006297915110012/METRICS.

[30] Kim JA, Ahn BN, Kong CS, Kim SK. Anti-inflammatory action of sulfated glucosamine on cytokine regulation in LPS-activated PMA-differentiated THP-1 macrophages. doi:10.1007/s00011-011-0377-7.

[31] Eygeris Y, Patel S, Jozic A, Sahay G, Sahay G. Deconvoluting Lipid Nanoparticle Structure for Messenger RNA Delivery. Nano Letters. 2020 6;20(6):4543–4549. Available from: https://pubs.acs.org/doi/full/10.1021/acs.nanolett.0c01386. doi:10.1021/ACS.NANOLETT.0C01386/ASSET/IMAGES/LARGE/NL0C01386_0005.JPEG.

[32] Veronese FM, Mero A. The impact of PEGylation on biological therapies. BioDrugs : clinical immunotherapeutics, biopharmaceuticals and gene therapy. 2008;22(5):315–329. Available from: https://pubmed.ncbi.nlm.nih.gov/18778113/. doi:10.2165/00063030-200822050-00004.

[33] McKinnon KM. Flow Cytometry: An Overview. Current protocols in immunology. 2018 2;120:5.1.1. Available from: /pmc/articles/PMC5939936/ /pmc/articles/PMC5939936/?report=abstract https://www.ncbi.nlm.nih.gov/pmc/articles/PMC5939936/. doi:10.1002/CPIM.40.